UCSF
UC San Francisco Electronic Theses and Dissertations

Title

PI3K/mTOR, microRNAs, and feed forward loops all stabilize MYCN protein in neuroblastoma; Paracrine signaling by MYCN subsequently drives angiogenesis

Permalink

https://escholarship.org/uc/item/91n0f24m

Author

Chanthery, Yvan Hathu

Publication Date

2011

Peer reviewed|Thesis/dissertation

PI3K/mTOR, microRNAs, and feed forward loops
all stabilize MYCN protein in neuroblastoma;
Paracrine signaling by MYCN subsequently drives
angiogenesis

by

Yvan Hathu Chanthery

DISSERTATION

Submitted in partial satisfaction of the requirements for the degree of

DOCTOR OF PHILOSOPHY

in

Biomedical Sciences

in the

GRADUATE DIVISION

of the

UNIVERSITY OF CALIFORNIA, SAN FRANCISCO

This work is dedicated to my parents and mentors, who have many important influences on my education and beyond.

Acknowledgements

I am truly grateful for all of the people are in my life, and all who have helped me throughout my graduate education at UCSF. First, I would like to thank my thesis advisor, Bill Weiss. I am forever indebted to him for everything he has done for me. He has provided a tremendous amount of guidance and support during my years in his lab. He also showed such great patience and understanding. He is one of my most important mentors, and an incredible influence in my graduate education and life.

I also would like to thank my qualifying exam and thesis committee members, who provided substantial amount of insights and advices into my projects. Zena Werb, the committee chair, has provided crucial insights and advices for my project. Zena is someone I have always idolized, especially for her role as an advocate for the advancement of women in science. Thiennu Vu is brilliant, yet very kind, personable and compassionate; she is a role model, and a great friend. Graeme Hodgson has taught me many essential assays for my projects. Peter Ralston is a great teacher and educator; the opportunity to teach along side with him is one of the most memorable experiences at UCSF.

Finally, I am very blessed to have a tremendous amount of love and support from my family and love ones. My parents have sacrificed everything for me so I could pursue my education and my interest in science. They are the source of unconditional love, and I am forever grateful and indebted. I would like to thank my significant other, Derrick Truong. He has always been there for me through all obstacles, and is the source of encouragement and inspiration. He has made every moment of my life so wonderful and amazing.

Abstract

The *MYCN* transcription factor and proto-oncogene contributes to a broad range of pediatric tumors including neuroblastoma, the most common extracranial solid tumor of childhood. Amplification of *MYCN* occurs in ~25% of neuroblastoma and is associated with high-risk disease in which survival is less than 20%. Tumor angiogenesis is prominent in neuroblastoma and contributes to metastasis, with increased microvascular density also associated inversely with survival.

We hypothesize that angiogenesis in neuroblastoma is triggered in-part by MYCN, that stabilization of MYCN is enhances by PI3K/mTOR and miR-17~92 activations, and that destabilization of MYCN contributes to the efficacy of PI3K inhibitors. In the first part, we show that NVP-BEZ235 decreased angiogenesis and tumor progression. Using both gain and loss of function approaches, we validate that the efficacy of NVP-BEZ235 depends greatly on stability of MYCN.

In the second part, we demonstrate that MYCN stability is enhanced through activation of miR-17~92 (a transcriptional target of MYCN); this in-turn induces a feed forward loop, leading to a highly aggressive pathology of MYCN-driven neuroblastoma. Altogether, these observations argue that NVP-BEZ235 should be tested in children with high-risk, *MYCN* amplified cancers.

TABLE OF CONTENTS

LIST OF FIGURES

Chapter 2:

CHAPTER 1: INTRODUCTION

Neuroblastoma, a tumor of peripheral neural crest origin, is the most common extracranial solid tumor of childhood. Patients with high-risk neuroblastoma typically have 43% five-year survival, followed by relapse and death (*1*). Cancer patients, especially infants and young children, are at high risk for long-term disability and toxicity from the late effects of conventional treatments (such as surgery, intensive radiation therapy and chemotherapy) (*2*). Hence, there is an urgent need to identify and utilize target-specific therapeutic approaches to reduce toxicity, and to improve survival as well as quality of life after treatment.

High-risk neuroblastoma is often associated with amplification of the transcription factor *MYCN* (*3, 4*). *MYCN,* a member of the Myc family, is amplified in 25% of all neuroblastoma tumors, and is a genetic marker for unfavorable pathology, associated with treatment failure (*5*). Amplification of *MYCN* is also a strong predictor of tumor progression, relapse, and disease-related mortality (*6*).

In embryonic development, *MYCN* is essential for neurogenesis and migration of peripheral neural crest (*7*). Constitutive inactivation of *MYCN* leads to embryonic lethality in mice (*8*). The expression of MYCN in adults, however, is extremely limited(*9*). Expression of MYCN is restricted postnatally, along with the amplification of MYCN in high-risk neuroblastoma, suggest MYCN as a biomarker and a potential therapeutic target.

1

To examine MYCN as a potential therapeutic target in vivo, we have previously generated a model for high-risk neuroblastoma by directing expression of a *MYCN* transgene to the peripheral neural crest of genetically engineered mice (GEM), under control of the rat Tyrosine Hydroxylase (TH) promoter (*10*). These murine tumors closely recapitulate human high-risk neuroblastoma both histologically and genetically and, like their human counterparts, are highly vascular (*11*).

In human neuroblastoma, amplification of *MYCN* also correlates with increased tumor-microvascular density, leading to aggressive disease, unfavorable histopathology, and poor survival (*12*). Further, previous study showed that, in xenografts, *MYCN*-amplified neuroblastoma cells induce robust angiogenesis in comparison with non-amplified cells *(13)*. Possible mechanisms through which MYCN could induce angiogenesis include deregulation of pro-angiogenic factors, which then recruit endothelial cells. However, a direct role for MYCN in regulating angiogenesis has not yet been demonstrated, though a number of basic observations suggest such a role for *c-myc*, a gene related to *MYCN*. Embryos from *c-myc* knockout mice show defective vasculogenesis, with tumors derived from c-*myc* knockout ES cells showing poor vascularization (*14*). The vascular endothelial growth factor (VEGF) family has emerged as a key regulator of angiogenesis in cancers including neuroblastoma (*15, 16*). A *c-myc* transgene targeted to the epidermis of transgenic mice led to skin tumors, with angiogenesis in these

lesions dependent on VEGF (*17*).   MYCN may similarly regulate angiogenesis, as MYCN can indirectly induce VEGF in cultured neuroblastoma cells (*18, 19*).

Since both c-myc and MYCN contribute to the regulation of VEGF and of angiogenesis, can clinical small molecule inhibitors that block MYCN or c-myc therefore be used to block angiogenesis? Like c-myc, MYCN is stabilized by activation of lipid kinase phosphoinositide 3'-kinase (PI3K) (*20*), with blockade of PI3K leading to decreased secretion of VEGF and decreased levels of MYCN protein (*18, 21, 22*). PI3K is a major downstream effector of Receptor Tyrosine Kinase (RTK) signaling; PI3K propagate downstream signals, including activation of Akt and mTOR, which in turn phosphorylates and inactivates glycogen synthase kinase 3-beta (GSK3β), a kinase that phosphorylates MYCN (*21, 23*). Phophorylate Inhibition of PI3K leads to destabilization of MYCN via proteasomal degradation.   When PI3K (or downstream signals Akt/mTOR) is blocked, GSK3β is activated, driving phosphorylation of MYCN protein. Phosphorylated MYCN is ubiquinated by E3 ubiquitin ligases and degraded in the proteasome (*24*). Thus, active PI3K signaling stabilizes MYCN protein, while blockade of PI3K leads to destabilization (*21, 24*).

Although MYCN activation in neuroblastoma leads to cell-cycle entry and proliferation of tumor cells (*25*), secondary apoptotic blockade is often

3

necessary for unregulated tumor growth and malignancy. What genetic or epigenetic events contribute to blockade of apoptosis in the progression of neuroblastoma? Both c-myc and *MYCN* induce the expression of six microRNAs in the miR-17~92 cluster (miR-17, 18a, 19a, 19b, 20a and 92-1) by binding to E-box recognition sites in the promoter of this cluster (*26, 27*). MicroRNAs (miRs) are 21-23 nucleotide non-coding RNAs. Together with a complex of associated protein known as RNA-induced silencing complex (RISC), miRNAs bind to sites in the 3'untranslated regions of mRNAs, and regulate gene expression by interfering with translation and stability of target mRNAs (*28, 29*). MicroRNAs of the miR-17~92 cluster act as oncogenes by promoting proliferation and suppressing apoptosis (*26, 30, 31*). In addition, miR-17~92 may also contribute to angiogenesis by suppressing anti-angiogenic factors, augmenting angiogenesis in cancer (*26*). Thus, PI3K and MYCN-induced miR-17~92 also represent attractive targets for therapy.

While we and others have shown previously that inhibitors of PI3K might block angiogenesis in MYCN driven neuroblastoma, whether this blockade is in-part dependent on MYCN is complicated by the fact that inhibitors of PI3K/ mTOR can block angiogenesis directly [through inhibition of PI3K in endothelial cells (*32*)], and by blocking fibroblasts and immune components of the tumor microenvironment, all of which contribute to angiogenic signaling [reviewed in (*16*)]. In Chapter 2, we evaluate a role for PI3K blockade as a translational approach to block angiogenesis in neuroblastoma. NVP-BEZ235

(Novartis) is an ATP-competitive clinical inhibitor of PI3K/mTOR with established preclinical anti-angiogenic and is now in Phase II trials in breast cancer (*33*). Treating both mice transgenic for TH-*MYCN* and an orthotopic primary human neuroblastoma (from a heavily pretreated patient with relapsed *MYCN*-amplified disease), we show that NVP-BEZ235 led to decreased angiogenesis and to improved survival. We demonstrate further that NVP-BEZ235 treatment destabilized MYCN, through blocking proteolytic degradation of MYCN protein. Degradation of MYCN was central to NVP-BEZ235-driven angiogenic blockade, resulting in decreased paracrine VEGF signaling between tumor and vascular cells. These studies suggest a role for dual PI3K/mTOR inhibitors in the clinical treatment of MYCN-driven cancers including neuroblastoma; and uncover a novel mechanism through which a clinical PI3K/mTOR inhibitor drives degradation of MYCN in tumor cells, with secondary blockade of vascular cells in the tumor microenvironment.

In Chapter 3, we examine how *MYCN*-amplified neuroblastoma cells activate PI3K signaling, even in the absence of known activating mutations in PI3K or downstream effectors. As mentioned above, miR-17~92 cluster is regulated by *MYCN*. Here, we demonstrate that miR-17~92 targets PTEN (a negative regulator of PI3K), stabilizing MYCN, and driving a feed-forward loop. By using anti-miR approaches in cell lines, and in mouse models, we further evaluate the efficacy and the therapeutic potential of anti-miR delivery system in neuroblastoma.

REFERENCES

1. R. E. Goldsby, K. K. Matthay, Neuroblastoma: evolving therapies for a disease with many faces. *Paediatr Drugs* **6**, 107 (2004).

2. T. Perwein, H. Lackner, P. Sovinz, M. Benesch, S. Schmidt, W. Schwinger, C. Urban, Survival and late effects in children with stage 4 neuroblastoma. *Pediatr Blood Cancer*).

3. G. M. Brodeur, Neuroblastoma: biological insights into a clinical enigma. *Nat Rev Cancer* **3**, 203 (2003).

4. J. M. Maris, The biologic basis for neuroblastoma heterogeneity and risk stratification. *Curr Opin Pediatr* **17**, 7 (2005).

5. J. M. Maris, Recent advances in neuroblastoma. *N Engl J Med* **362**, 2202).

6. G. M. Brodeur, R. C. Seeger, M. Schwab, H. E. Varmus, J. M. Bishop, Amplification of N-myc in untreated human neuroblastomas correlates with advanced disease stage. *Science* **224**, 1121 (1984).

7. P. S. Knoepfler, P. F. Cheng, R. N. Eisenman, N-myc is essential during neurogenesis for the rapid expansion of progenitor cell populations and the inhibition of neuronal differentiation. *Genes Dev* **16**, 2699 (2002).

8. J. Charron, B. A. Malynn, P. Fisher, V. Stewart, L. Jeannotte, S. P. Goff, E. J. Robertson, F. W. Alt, Embryonic lethality in mice homozygous for a targeted disruption of the N-myc gene. *Genes Dev* **6**, 2248 (1992).

9. I. Semsei, S. Y. Ma, R. G. Cutler, Tissue and age specific expression of the myc proto-oncogene family throughout the life span of the C57BL/6J mouse strain. *Oncogene* **4**, 465 (1989).

10. W. A. Weiss, K. Aldape, G. Mohapatra, B. G. Feuerstein, J. M. Bishop, Targeted expression of MYCN causes neuroblastoma in transgenic mice. *EMBO J* **16**, 2985 (1997).

11. C. S. Hackett, J. G. Hodgson, M. E. Law, J. Fridlyand, K. Osoegawa, P. J. de Jong, N. J. Nowak, D. Pinkel, D. G. Albertson, A. Jain, R. Jenkins, J. W. Gray, W. A. Weiss, Genome-wide array CGH analysis of murine neuroblastoma reveals distinct genomic aberrations which parallel those in human tumors. *Cancer Res* **63**, 5266 (2003).

12. D. Meitar, S. E. Crawford, A. W. Rademaker, S. L. Cohn, Tumor angiogenesis correlates with metastatic disease, N-myc amplification, and poor outcome in human neuroblastoma. *J Clin Oncol* **14**, 405 (1996).

13. D. Ribatti, L. Raffaghello, F. Pastorino, B. Nico, C. Brignole, A. Vacca, M. Ponzoni, In vivo angiogenic activity of neuroblastoma correlates with MYCN oncogene overexpression. *Int J Cancer* **102**, 351 (2002).

14. T. A. Baudino, C. McKay, H. Pendeville-Samain, J. A. Nilsson, K. H. Maclean, E. L. White, A. C. Davis, J. N. Ihle, J. L. Cleveland, c-Myc is

essential for vasculogenesis and angiogenesis during development and tumor progression. *Genes Dev* **16**, 2530 (2002).

15. R. H. Gold, Indications and risk-benefit of mammography. *J Fam Pract* **8**, 1135 (1979).

16. A. S. Chung, J. Lee, N. Ferrara, Targeting the tumour vasculature: insights from physiological angiogenesis. *Nat Rev Cancer* **10**, 505).

17. U. E. Knies-Bamforth, S. B. Fox, R. Poulsom, G. I. Evan, A. L. Harris, c-Myc interacts with hypoxia to induce angiogenesis in vivo by a vascular endothelial growth factor-dependent mechanism. *Cancer Res* **64**, 6563 (2004).

18. J. Kang, P. G. Rychahou, T. A. Ishola, J. M. Mourot, B. M. Evers, D. H. Chung, N-myc is a novel regulator of PI3K-mediated VEGF expression in neuroblastoma. *Oncogene* **27**, 3999 (2008).

19. A. Lasorella, G. Rothschild, Y. Yokota, R. G. Russell, A. Iavarone, Id2 mediates tumor initiation, proliferation, and angiogenesis in Rb mutant mice. *Mol Cell Biol* **25**, 3563 (2005).

20. A. M. Kenney, H. R. Widlund, D. H. Rowitch, Hedgehog and PI-3 kinase signaling converge on Nmyc1 to promote cell cycle progression in cerebellar neuronal precursors. *Development* **131**, 217 (2004).

21. L. Chesler, C. Schlieve, D. D. Goldenberg, A. Kenney, G. Kim, A. McMillan, K. K. Matthay, D. Rowitch, W. A. Weiss, Inhibition of phosphatidylinositol 3-kinase destabilizes MYCN protein and blocks malignant progression in neuroblastoma. *Cancer Res* **66**, 8139 (2006).

22. J. I. Johnsen, L. Segerstrom, A. Orrego, L. Elfman, M. Henriksson, B. Kagedal, S. Eksborg, B. Sveinbjornsson, P. Kogner, Inhibitors of mammalian target of rapamycin downregulate MYCN protein expression and inhibit neuroblastoma growth in vitro and in vivo. *Oncogene* **27**, 2910 (2008).

23. L. C. Cantley, The phosphoinositide 3-kinase pathway. *Science* **296**, 1655 (2002).

24. M. Welcker, B. E. Clurman, FBW7 ubiquitin ligase: a tumour suppressor at the crossroads of cell division, growth and differentiation. *Nat Rev Cancer* **8**, 83 (2008).

25. C. Schorl, J. M. Sedivy, Loss of protooncogene c-Myc function impedes G1 phase progression both before and after the restriction point. *Mol Biol Cell* **14**, 823 (2003).

26. M. Dews, A. Homayouni, D. Yu, D. Murphy, C. Sevignani, E. Wentzel, E. E. Furth, W. M. Lee, G. H. Enders, J. T. Mendell, A. Thomas-Tikhonenko, Augmentation of tumor angiogenesis by a Myc-activated microRNA cluster. *Nat Genet* **38**, 1060 (2006).

27. J. H. Schulte, S. Horn, T. Otto, B. Samans, L. C. Heukamp, U. C. Eilers, M. Krause, K. Astrahantseff, L. Klein-Hitpass, R. Buettner, A. Schramm, H. Christiansen, M. Eilers, A. Eggert, B. Berwanger, MYCN

regulates oncogenic MicroRNAs in neuroblastoma. *Int J Cancer* **122**, 699 (2008).

28. J. T. Mendell, miRiad roles for the miR-17-92 cluster in development and disease. *Cell* **133**, 217 (2008).

29. G. Stefani, F. J. Slack, Small non-coding RNAs in animal development. *Nat Rev Mol Cell Biol* **9**, 219 (2008).

30. L. He, J. M. Thomson, M. T. Hemann, E. Hernando-Monge, D. Mu, S. Goodson, S. Powers, C. Cordon-Cardo, S. W. Lowe, G. J. Hannon, S. M. Hammond, A microRNA polycistron as a potential human oncogene. *Nature* **435**, 828 (2005).

31. K. A. O'Donnell, E. A. Wentzel, K. I. Zeller, C. V. Dang, J. T. Mendell, c-Myc-regulated microRNAs modulate E2F1 expression. *Nature* **435**, 839 (2005).

32. H. P. Gerber, A. McMurtrey, J. Kowalski, M. Yan, B. A. Keyt, V. Dixit, N. Ferrara, Vascular endothelial growth factor regulates endothelial cell survival through the phosphatidylinositol 3'-kinase/Akt signal transduction pathway. Requirement for Flk-1/KDR activation. *J Biol Chem* **273**, 30336 (1998).

33. S. M. Maira, F. Stauffer, J. Brueggen, P. Furet, C. Schnell, C. Fritsch, S. Brachmann, P. Chene, A. De Pover, K. Schoemaker, D. Fabbro, D. Gabriel, M. Simonen, L. Murphy, P. Finan, W. Sellers, C. Garcia-Echeverria, Identification and characterization of NVP-BEZ235, a new orally available dual phosphatidylinositol 3-kinase/mammalian target of rapamycin inhibitor with potent in vivo antitumor activity. *Mol Cancer Ther* (2008).

CHAPTER 2: Paracrine signaling through MYCN enhances tumor-vascular interactions in neuroblastoma

Source: The following chapter contains unpublished manuscript that has been submitted to Science: Translational Science Journal.

Paracrine signaling through MYCN enhances tumor-vascular interactions in neuroblastoma

Yvan H. Chanthery[1-4], W. Clay Gustafson[2-5], Melissa Itsara[2-5], Anders Persson[2-5],
Christopher S. Hackett[1-4], Matt Grimmer[2-5], Elise Charron[2-5], Slava Yakovenko[2-5],
Grace Kim[6], Katherine K. Matthay[2-5] and William A. Weiss[1-5*]

ABSTRACT

Neuroblastoma, a tumor of peripheral neural crest origin, numbers among the most common childhood cancers. Both amplification of the proto-oncogene *MYCN* and increased neo-angiogenesis mark high-risk disease. Since angiogenesis is regulated by phosphatidylinositol-3' kinase (PI3K), we tested a clinical PI3K inhibitor, NVP-BEZ235, in *MYCN*-dependent neuroblastoma. NVP-BEZ235 decreased angiogenesis and improved survival in both primary human (recurrent *MYCN*-amplified orthotopic xenograft) and transgenic mouse models for *MYCN*-driven neuroblastoma. Using both gain and loss of function approaches, we demonstrate that the anti-angiogenic efficacy of NVP-BEZ235 depends critically on MYCN *in vitro* and *in-vivo*. Thus, clinical PI3K/mTOR inhibitors drive degradation of MYCN in tumor cells, with secondary paracrine blockade of angiogenesis. These observations argue that NVP-BEZ235 should be tested in children with high-risk, *MYCN* amplified neuroblastoma.

INTRODUCTION

Neuroblastoma, a tumor of peripheral neural crest origin, is the most common extracranial solid tumor of childhood. *MYCN,* a Myc family proto-oncogene, is amplified in 25% of neuroblastoma tumors, and is a genetic marker for treatment failure in this disease (*1*). We have previously generated a model for high-risk neuroblastoma by directing expression of a *MYCN* transgene to the peripheral neural crest of genetically engineered mice (GEM), under control of the rat Tyrosine Hydroxylase (TH) promoter (*2*). These murine tumors closely recapitulate human high-risk neuroblastoma both histologically and genetically and, like their human counterparts, are highly vascular (*3*).

The vascular endothelial growth factor (VEGF) family has emerged as a key regulator of angiogenesis in cancers including neuroblastoma, correlating with unfavorable histology and aggressive behavior (*6, 7*). MYCN may regulate angiogenesis, as MYCN can indirectly induce VEGF in cultured neuroblastoma cells (*9, 10*). Since MYCN contribute to the regulation of VEGF and of angiogenesis, can clinical small molecule inhibitors that block MYCN therefore be used to block angiogenesis? the design of clear experiments is complicated by the fact that inhibitors of PI3K and mTOR can block angiogenesis directly [through inhibition of PI3K in endothelial cells (*14*)], and by blocking fibroblasts and immune components of the tumor microenvironment, all of which contribute to angiogenic signaling [reviewed in (*7*)].

Here, we evaluate a role for PI3K blockade as a translational therapeutic approach to inhibit tumor-vascular interactions in neuroblastoma, incorporating multiple genetic strategies to distinguish direct effects of these interventions on vascular cells, from paracrine effects of tumor cells on endothelial cells. These studies demonstrate that MYCN is a critical target for PI3K inhibitors, as blockade of MYCN contributes prominently to the antiangiogenic effects of this class of compounds.

RESULTS

A dual PI3K/mTOR inhibitor enhances survival and suppresses tumor burden in GEM and orthotopic xenograft models of MYCN-driven neuroblastoma.

To clarify whether *MYCN* amplification sensitizes tumor cells to dual inhibitors of PI3K and mTOR, we treated a panel of *MYCN*-amplified and non-amplified human neuroblastoma-derived cell lines with the PI3K/mTOR inhibitor NVP-BEZ235 (Fig. 2-1 A&B). These data suggest *MYCN* amplification as a biomarker for tumor aggressiveness, and for relative sensitivity to NVP-BEZ235.

We next used mice transgenic for TH-*MYCN* as a platform to test the efficacy of PI3K/mTOR inhibition in-vivo. Upon detection of tumors by palpation (mean age 60d), tumor-bearing mice transgenic for TH-*MYCN* were treated with daily oral gavage of NVP-BEZ235 (35mg/kg) or vehicle control for 28d (Fig. 2-2A). Notably, vehicle treated animals showed significant mortality starting 21d after initiating treatment, while animals receiving active agent remained alive throughout the treatment period. To determine whether active therapy led to durable remission, NVP-BEZ235 was discontinued after 28d (arrow in Fig. 2-2 A). Within 3 weeks of initial tumor detection, most of control animals required sacrifice due to signs of advanced disease (Fig. 2-2A). From the

time of tumor detection to sacrifice, drug-treated mice survived an average of ~1.5-fold longer than animals receiving vehicle alone.

We validated this in-vivo result by orthotopic transplantation of a recurrent *MYCN*-amplified primary human tumor (SFNB-06) into the kidney capsule of nude mice. Mice were treated at 3d post transplant with daily oral gavage of NVP-BEZ235 (35mg/kg) or vehicle control for 28d (arrow in Fig. 2-2B). NVP-BEZ235 treatment again significantly improved overall survival (Fig. 2-2B).

We also demonstrated that NVP-BEZ235 significantly inhibited tumor burden in mice transgenic for TH-*MYCN,* and in mice carrying orthotopic xenografts of SFNB-06 primary tumors. Tumor volume was measured in mice at the time of initial palpation (prior to treatment) and again after daily treatment with vehicle or NVP-BEZ235 (14d). Tumor burden was calculated by comparing the initial volume to the end-volume in treatment and control groups (Fig. 2-3A&B). All animals survived therapy without measurable weight loss (not shown). Full necropsies revealed no abnormalities apart from those documented in tumors.

A dual PI3K/mTOR inhibitor suppresses tumor proliferation and angiogenesis

Given the known role for NVP-BEZ235 in blocking angiogenesis (*15*), we further analyzed GEM and orthotopic neuroblastomas for vascular complexity. TH-MYCN tumors and SNFB-06 orthotopic xenografts (from Fig. 2-3) were collected and analyzed. NVP-BEZ235 induced a significant reduction in vascular density within tumors in both models, as indicated by CD31 endothelial cell staining (Fig. 2-4A,E and Fig. 2-5A,E).

Hematoxylin and eosin staining showed reduced vascular density in the NVP-BEZ235 treatment arms in both models (Fig. 2-4D,H,I and Fig. 2-5D,H,I). Animals treated with NVP-BEZ235 also showed decreased perivascular cell coverage (α-SMA staining) in both TH-*MYCN* and human orthotopic mouse models (Fig. 2-4B,F, I and Fig 2-5B,F, I respectively). Further, NVP-BEZ235 affected tumor cells directly, leading to decreased proliferation in both TH-*MYCN* and SFNB-06 tumors (Fig. 2-4C, G, I and Fig. 2-5C, G, I). Similar histological changes were observed after either 7d or 28d treatment with NVP-BEZ235 (not shown). Importantly, NVP-BEZ235 had no appreciable effect on established retinal vasculature in control animals, consistent with a therapeutic index for PI3K/mTOR inhibition on tumor-associated vessels, relative to normal, established vasculature (Fig. 2-6A&B). Rapid revascularization followed drug withdrawal, concomitant with tumor growth and overall mortality (Fig. 2-7A-C). These data show that NVP-BEZ235

treatment reversibly reduced vascularity and inhibited proliferation of *MYCN*-driven neuroblastoma tumors *in vivo.*

Inhibition of PI3K/mTOR leads to decreased levels of MYCN protein

We next analyzed PI3K and mTOR signaling in tumor extracts from mice treated with drug for 7d or 14d. NVP-BEZ235 treatment of both mouse and human neuroblastoma was associated with reduced levels of MYCN protein, correlating with reduced phosphorylation of the PI3K target Akt, and of the mTOR target p-rpS6 (Fig. 2-8A&B). After 14d treatment, levels of MYCN mRNA were not significantly changed (Fig. 2-9A&B) consistent with NVP-BEZ235 blocking MYCN post-transcriptionally.

MYCN in tumor cells contributes to paracrine signaling between tumor and endothelial cells: genetic studies

To test whether PI3K-driven stabilization of MYCN contributed functionally to the tumor vascular microenvironment, we transduced SHEP human neuroblastoma cells (which have no detectable MYCN) with retroviral vectors expressing wild-type murine MYCN *(MYCN^{WT})* or a phospho-mutant of *MYCN (MYCN^{T58A})* that is resistant to inhibitors of PI3K and of mTOR (*11, 12, 16*). As control, we also transduced SHEP with control-vector expressing GFP; these cells responded similarly to parental SHEP shown in Fig. 2-1 (Fig. 2-10). We first confirmed that *MYCN^{T58A}* protein was stabilized by

cycloheximide pulse chase assay, with vehicle control or NVP-BEZ235 (Fig. 2-11A&B). $MYCN^{T58A}$ protein conferred resistance to treatment with NVP-BEZ235, even in the setting of effective inhibition of downstream Akt and rpS6 phosphorylation (Fig. 2-12). The ability of NVP-BEZ235 to block proliferation and viability was accordingly blunted in $MYCN^{T58A}$ cells as compared with $MYCN^{WT}$ cells (Fig. 2-13).

Since NVP-BEZ235 destabilizes MYCN protein in tumor cells and blocks neuroblastoma angiogenesis *in vivo*, we hypothesized that MYCN may be responsible for paracrine signaling between tumors and vasculature. To determine whether blockade of MYCN in tumor cells contributed to paracrine signaling between tumor and vascular cells, we next co-cultured human umbilical vein endothelial cells (HUVEC) with $MYCN^{WT}$ or with $MYCN^{T58A}$ tumor cells. HUVEC were plated in the top of a Boyden Chamber, with neuroblastoma cells plated at the bottom. Migration of HUVEC was proportional to the level of MYCN in co-cultured neuroblastoma cells, with minimal migration in $MYCN$ negative cells (Fig. 2-14), modest migration in $MYCN^{WT}$ cells, and further HUVEC migration in $MYCN^{T58A}$ cells, but insignificantly different than $MYCN^{WT}$ (Fig. 2-15). $MYCN^{T58A}$ cells were relatively less sensitive to NVP-BEZ235, with sustained migration of HUVECs, as compared to limited migration of HUVEC co-cultured with $MYCN^{WT}$ cells (Fig. 2-15). These findings, along with control HUVEC migration in SHEP vector-GFP control cells (Fig. 2-14) are consistent with a

component of HUVEC migration being regulated partially by PI3K in endothelial cells or by non-MYCN dependent pathway (*17-19*).   In addition, our genetic experiments demonstrate a significant difference in HUVEC migration, comparing $MYCN^{T58}$ and $MYCN^{WT}$ cells in NVP-BEZ235 treatment arms, suggesting that a significant fraction of HUVEC migration is driven by *MYCN*-dependent signaling between tumor and HUVEC cells (Fig. 2-15).

In light of the known importance of VEGF in angiogenesis, we analyzed the effects of NVP-BEZ235 on VEGF production and secretion.   Secretion of VEGF was increased in cells transduced with $MYCN^{T58A}$ as compared to $MYCN^{WT}$, and was nearly absent in negative control SHEP cells (not shown). Treatment with NVP-BEZ235 reduced secretion of VEGF by 30% in $MYCN^{WT}$ cells, compared with 10% reduction in $MYCN^{T58A}$ cells (Fig. 2-16A). Analysis by real-time qRT-PCR showed that NVP-BEZ235 treatment minimally affected levels of VEGF mRNA in $MYCN^{T58A}$ cells while significantly reducing levels of VEGF mRNA in $MYCN^{WT}$ cells, consistent with transcriptional regulation of VEGF downstream of MYCN (Fig. 2-16B). In cycloheximide pulse chase assay, we further verified that MYCN does not regulate VEGF at the post-transcription level, as neither $MYCN^{T58A}$ nor treatment with NVP-BEZ235 affected the half-life of VEGF protein (Fig. 2-17).   To extend this result, we analyzed treated tumors from mice transgenic for TH-*MYCN* and from orthotopic xenografts of SFNB-06, verifying that NVP-BEZ235 treatment was associated with decreased levels of both VEGF protein and VEGF

mRNA *in vivo* (Fig. 2-18A&B).

Knockdown of MYCN substantiates a role in paracrine signaling

To further evaluate a role for MYCN in paracrine signaling between tumor and vascular cells, we next analyzed *MYCN*-amplified Kelly neuroblastoma cells, comparing the effect of NVP-BEZ235 with shRNA directed against MYCN. Knockdown of MYCN resulted in decreased abundance of MYCN protein, with potency equivalent to or increased compared with NVP-BEZ235 treatment, and additive in combination (Fig. 2-19A&B). Proliferation and viability of tumor cells decreased proportionately with decreasing levels of MYCN protein in cells treated with shRNA against MYCN, NVP-BEZ235, or in response to both interventions, resulting in a cooperative response (Fig. 2-20A). MYCN knockdown and treatment with NVP-BEZ235 also attenuated levels of VEGF secretion and VEGF mRNA (Fig. 2-20B&C). Importantly, reduced MYCN protein in tumor cells also resulted in subsequent inhibition of migration in co-cultured HUVEC cells (Fig. 2-20B). These data validate a role for MYCN in directing paracrine signaling from tumor cells to endothelial cells in neuroblastoma.

A doxycycline-inducible allele verifies a role for MYCN in tumor-vascular interactions.

To further clarify *MYCN*-dependent versus *MYCN*-independent roles of NVP-

BEZ235 on both tumor and endothelial cells we used SHEP-TET21/N, a human neuroblastoma cell line in which transcription of MYCN can be toggled "off" or "on" by the addition of doxycycline (dox) to the media (20) (Fig. 2-21A). As expected, NVP-BEZ235 treatment destabilized MYCN in TET21/N cells (Fig. 2-21B). Dox led to reduction of MYCN with significantly decreased proliferation and viability, as compared to MYCN-"on" cells (Fig. 2-22A). NVP-BEZ235 treatment reduced proliferation and viability in MYCN "on" cells to levels comparable to MYCN "off" cells, with no significant effect on proliferation and a modest effect on viability in MYCN "off" cells (Fig. 2-22A).

Dox-regulated suppression of MYCN transcription also inhibited VEGF secretion by 70%, compared to levels in MYCN "on" cells, and attenuated migration of co-cultured HUVEC cells (Fig. 2-22A). We excluded an off-target effect of dox on viability by treating HUVECs with dox directly (Fig. 2-22B). NVP-BEZ235 treatment of MYCN "on" cells also reduced VEGF secretion and HUVEC migration to baseline levels. Similar treatment of MYCN "off" cells showed no significant effect on secretion of VEGF, and modest effects on migration (Fig. 2-22A). These data again show that MYCN promotes angiogenesis by augmenting paracrine crosstalk between tumor cells and endothelial cells in the microenvironment. Targeting MYCN at the mRNA level (through addition of dox in TET21/N cells, or by transducing shRNA in Kelly cells) or at the protein level (using NVP-BEZ235) abrogates this MYCN-dependent paracrine signaling and contributes to angiogenic collapse.

Impairing E3-ligase dependent degradation of MYCN in tumor cells promotes resistance to NVP-BEZ235

To further evaluate the importance of MYCN degradation to the action of NVP-BEZ235, we used shRNA in *MYCN*-amplified Kelly cells to knock-down HUWE1 (Fig. 2-23A), an ubiquitin ligase known to degrade T58 phosphorylated MYCN protein (*21, 22*)). MYCN protein accumulated in cells depleted for HUWE1, with no clear changes noted in PI3K/mTOR signaling (Fig. 2-23A&B). HUWE1 knockdown also prolonged the half-life of MYCN protein (Fig. 2-23C), and mediated resistance to NVP-BEZ235-induced degradation of MYCN as compared to shRNA-control cells (Fig. 2-23B).

We next investigated whether stabilization of MYCN (in response to HUWE1 knock-down) could antagonize the effects of NVP-BEZ235 on tumor cells. Knockdown of HUWE1 and subsequent stabilization of MYCN partially attenuated the effects of NVP-BEZ235 on proliferation and viability of tumor cells (~30% reduction), compared to similar treatment of tumor cells transduced with shRNA-control (>60% reduction, Fig. 2-24). Further, as control, knockdown of HUWE1 in *MYCN* non-amplified cells led to insignificant differences in viability and proliferation, comparing NVP-BEZ235 and vehicle (Fig. 2-25A&B). We conclude that blocking the ubiquitination and subsequent proteolytic degradation of MYCN in neuroblastoma cells attenuates the effects of NVP-BEZ235 on proliferation and survival.

Impairing E3-ligase dependent degradation of MYCN in tumor cells partially rescues the anti-angiogenic effects of NVP-BEZ235

Next we assessed whether preventing HUWE1 dependent ubiquitination of MYCN could similarly attenuate the paracrine effects of NVP-BEZ235 on angiogenesis. We therefore co-cultured HUVEC with either HUWE1 knockdown or shRNA-control tumor cells, in the presence of either NVP-BEZ235 or vehicle. In the absence of NVP-BEZ235, both secretion of VEGF and migration of HUVEC were similar in HUWE1 knockdown compared with shRNA-control cells (Fig. 2-24). In treated cells, NVP-BEZ235 caused only 25% reduction in levels of VEGF in HUWE1-knockdown cells as compared with 60% in shRNA-control (Fig. 2-24). The efficacy of NVP-BEZ235 in blocking migration was significantly reduced in HUVEC co-cultured with HUWE1-knockdown cells (55% reduction), as compared with HUVEC co-cultured with control cells (75% reduction, Fig. 2-24). Thus, partial blockade of MYCN ubiquitination in tumor cells causes resistance to NVP-BEZ235, leading to decreased secretion of VEGF and decreased recruitment of endothelial cells. We conclude that MYCN represents a critical target of NVP-BEZ235 in tumor cells, resulting in reduced paracrine signaling to co-cultured HUVEC.

To extend these results, we transplanted both control and HUWE1-knockdown Kelly cells into renal capsules of nude mice for a cohort study.

Two weeks after transplantation, mice were treated with either vehicle or NVP-BEZ235 (35 mg/kg by daily oral gavage for 14d). HUWE1-knockdown tumors were comparable in weight to shRNA-control tumors (not shown). NVP-BEZ235 prevented progression of established tumors in control mice (Fig. 2-26). Importantly, the efficacy of NVP-BEZ235 in blocking tumor growth was markedly attenuated by knockdown of HUWE1 (Fig. 2-26A&B; 95% reduction combining NVP-BEZ235 with shRNA-control vs. 50% reduction combining NVP-BEZ235 with HUWE1 shRNA). These data demonstrate that attenuating the activity of NVP-BEZ235 against MYCN markedly reduced the activity of this drug against tumor cells.

Next, we evaluated the angiogenic microenvironment to determine whether HUWE1 knockdown in tumor cells affected response to NVP-BEZ235 in vascular cells. In response to vehicle, both shRNA-control and HUWE1 knockdown tumors were highly vascularized (Fig. 2-27A,C and M,O, quantitated in Q) with tumor cells showing prominent proliferation (Fig. 2-27E,G and Q). NVP-BEZ235 effectively blocked both formation of angiogenic blood vessels and proliferation of tumor cells in control mice (Fig. 2-27B,F,N,Q). The efficacy of NVP-BEZ235 in HUWE1-knock-down tumors was blunted markedly, with retention of both vascular networks and proliferating tumor cells (Fig. 2-27D,H,P, Q). These data suggest that stabilization of MYCN in tumor cells *in-vivo* reduces the potency of NVP-BEZ235 against both neuroblastoma tumors and vascular elements in the tumor

microenvironment. We conclude that MYCN protein represents a critical target for the efficacy of NVP-BEZ235 in neuroblastoma tumors driven by *MYCN,* and that destabilization of MYCN in tumor cells contributes prominently to the anti-angiogenic efficacy of NVP-BEZ235.

DISCUSSION

Amplification of *MYCN* is a genetic marker for high-risk neuroblastoma, also correlating with increased vascularity (*4*). The correlation of *MYCN* amplification with vascularity, and the demonstration that withdrawal of MYC in tumors driven by a MYC-ER fusion protein led to angiogenic collapse (*8*), suggest MYCN as a potential therapeutic target. Yet effective therapeutic blockade of MYCN and other transcription factors remains generally challenging. We previously demonstrated that tool-compound inhibitors of PI3K/mTOR can destabilize MYCN and can block proliferation of tumors driven by TH-MYCN (*12*). Others have validated these findings, and in addition demonstrated that these tool-compound inhibitors of PI3K/mTOR can block VEGF secretion (*9, 13*). These observations suggest that PI3K-driven blockade of MYCN (using clinical inhibitors) could cause angiogenesis inhibition.

Historically, the majority of translational therapeutic studies of cancer have been performed in xenograft models. While such models provide important insights, immunodeficient mice do not recapitulate the tumor microenvironment interaction seen in human disease. To study the intricacies of these interactions, we therefore demonstrated that the clinical agent NVP-BEZ235 drove angiogenic collapse in both orthotopic xenograft and transgenic models for *MYCN*-driven neuroblastoma *in-vivo.* We also xenografted two parental *MYCN* non-amplified cell lines and 1 non-amplified

human primary tumor, with no growth in-vivo by 3 months. Similar difficulties in xenografting *MYCN* non-amplified tumors have also been noted by others (*31*). Thus, we limit our *in-vivo* conclusions in this study to MYCN-driven disease.

The functional importance of MYCN as a target of NVP-BEZ235 is not fully clarified by our in-vivo studies however, since inhibitors of PI3K/mTOR can block endothelial cells directly (*14*), and can block tumor associated pericytes, immune cells and possibly extracellular matrix in the tumor microenvironment, all of which contribute to angiogenesis [reviewed in (*7*)]. Therefore, to clarify whether inhibition of MYCN in tumor cells contributed prominently to angiogenic collapse, we co-cultured endothelial cells with tumor cells using:

1). PI3K-resistant alleles (*MYCN^{T58A}*),

2). shRNA against amplified *MYCN* in human neuroblastoma cells;

3). A doxycycline-repressible allele of MYCN, and

4). shRNA against the ubiquitin ligase HUWE1.

These experiments collectively demonstrate that MYCN is a biomarker for relative sensitivity to PI3K/mTOR inhibitors, and that blockade of MYCN is critical to the anti-angiogenic effects of PI3K/mTOR inhibitors in neuroblastoma. Further, while overexpression of *MYCN* accelerated the growth of non-amplified neuroblastoma cells, it also sensitized these cells to NVP-BEZ235. These observations are consistent with findings that ectopic

expression of *MYCN* can sensitize cells to combination chemotherapy and targeted therapy, using Trail, doxorubicin, *ZVAD or* PI3K inhibitors (*28-30*).

To further verify MYCN as a critical target, we used HUWE1 knockdown tumor cells (deficient in PI3K/mTOR mediated MYCN proteolysis) to establish an orthotopic xenograft model, demonstrating that HUWE1 knockdown tumors were resistant to the anti-angiogenic activity of NVP-BEZ235. Even near complete knockdown of HUWE1 did not completely attenuate the efficacy of PI3K/mTOR inhibition, likely because additional ubiquitin ligases signal downstream of the PI3K/mTOR/MYCN pathway, including FBXW7, which also degrades MYCN in neuroblastoma (*23, 24*). FBXW7 also targets the mTOR protein (*25*), and is itself phosphorylated by PI3K (*26*). These complex   interactions make FBXW7 a poor candidate for interpreting knockdown studies that also incorporate PI3K/mTOR inhibitors.

Several paracrine effectors contribute to angiogenesis in neuroblastoma, (*32*). Our observations that blockade of MYCN led to reduction of VEGF *in-vitro* and *in-vivo* and to decreased migration of endothelial cells implicate VEGF signaling as one effector of tumor-vascular interactions, do not exclude roles for other paracrine factors, and do not exclude the fact that VEGF is also regulated through pathways independent of MYCN. To clarify mechanism, we showed that VEGF mRNA maybe regulated   transcriptionally through a MYCN-dependent   pathway.   This   finding   is   consistent   with   prior demonstrations that VEGF is an indirect target of MYCN (*10*) and that MYCN

cooperates with HIF1α to regulate angiogenesis and progression (*33*). Since PI3K and mTOR inhibitors can suppress HIF1α and other effectors of VEGF (*9, 10*) it is likely that NVP-BEZ235 regulates VEGF levels, HIF1α, and angiogenesis in both MYCN-dependent and independent manners.

In overview, our studies clarify that MYCN is a critical target of NVP-BEZ235, that inhibition of PI3K and mTOR signaling effect angiogenic blockade in-part through a MYCN-dependent pathway, and highlight the importance of paracrine MYC-directed signaling between tumor cells and vascular cells in this disease. Further, our studies argue that NVP-BEZ235 should be tested in children with high-risk, *MYCN*-amplified neuroblastoma tumors.

MATERIALS AND METHODS

In vivo experiments

TH-*MYCN* mice with tumors, detected by palpation (mean age at detection was 60 +/- 15d), were treated with NVP-BEZ235 (35 mg/kg in PEG300) or vehicle (PEG300), once daily by oral gavage, for 7d or 14d. Dosage and route of administration were by recommendation from Novartis. For western analysis and qRT-PCR, tumors were snap frozen. For immunohistochemistry, tumors and tissues were fixed and processed as described below. For tumor burden assessment, record of tumor were collected at t=0d before treatment, and again at t=14d, the last day of treatment.

Kidney Capsule Orthotopic Models

A human *MYCN*-amplified primary neuroblastoma tumor was obtained from a child with relapsed metastatic disease of the highest grade and stage (SFNB-06). Tumor pieces ($2mm^3$) were implanted into kidney capsule of nude mice. After 3 weeks when palpable tumors were detected, mice were treated with vehicle PEG300 or NVP-BEZ235 daily for 14d. Tumors were collected at the last day of treatment, weight and volume, were recorded, tissues were processed as below and histology was assessed.

For orthotopic kidney capsule experiments using human cell lines, neuroblastoma cells were resuspended in1:1 PBS+ Matrigel (BD Biosciences). Nude mice at 4-6 weeks of age were anesthetized with

isoflourane. Cells ($1*10^6$) were injected into kidney capsule. Two weeks after transplantation, mice were treated for 14d, and tumor weight and volume were record, and histology were processed as below.   All animals were handled in accordance with institutional LARC guidelines.

Survival Studies

TH-MYCN mice with palpable tumors were treated with NVP-BEZ235 (35 mg/kg in PEG300) or vehicle (PEG300), once daily for 28 days. Human primary SFNB-06 mice were treated once daily for 28d, starting 3 days after orthotopic transplantation, (dosage as above). Continuation of NVP-BEZ235 beyond 28 day was associated with dramatic weight loss due either to repeated gavage injury to the esophagus, or possibly from systemic toxicity (not shown), requiring cessation of treatment per IACUC guidelines.   All mice were monitored until euthanasia is required, in accordance with institutional IACUC guidelines.

Histology

For fluorescence microscopy, tissue and tumors were collected, fixed with 4% PFA overnight, cryoprotected with 30% sucrose, then OCT imbedded and frozen at -80° C. Sections (30 μm) were cut, mounted onto glass slides, blocked for 4h with 10% goat serum in PBST (PBS, 1% Triton X-100), and then incubated overnight at 4° C with primary antisera. Slides were washed with PBST for 1h, incubated for 4h with secondary antibodies, and mounted

31

with Flourmount G (Southern Biotech). Images were captured with Zeiss Axiophot fluorescence microscopes. Primary antibodies: monoclonal hamster anti-mouse CD31 (1:500, Chemicon) or monoclonal rat anti-mouse CD31 (1:500, Pharmingen/BD Bioscience),MYCN, VEGFA (1:500, Santa Cruz), and 5% normal goat serum (Invitrogen), mouse monoclonal Cy3-conjugated alpha-smooth muscle actin (α-SMA; 1:500, Sigma-Aldrich), rabbit anti-Ki67 (1:200, clone SP6, Lab Vision). Secondary: Alexa 488 goat anti-rat & goat anti-hamster IgGs or Alexa 568 goat anti-rabbit IgG (1:200; Molecular Probes/Invitrogen), DAPI Nucleic Acid Stain (1:1000; Molecular Probes/Invitrogen). All quantitations were done using ImageJ program (NIH).

For retinal studies, eyes were collected and fixed with 4% PFA. Dissected retinas were blocked with 5% mouse serum in PBST for 3 hr, and then incubated overnight at 4^OC with 25 mg/ml biotinylated isolectin B4 (Sigma) in PBLEC (1% Triton X-100, 0.1 mM $CaCl2$, 0.1 mM $MgCl2$, 0.1 mM $MnCl2$, in PBS [pH 6.8]). Retinas were then washed and stained with Alexa 488 streptavidin (Molecular Probes). Images of flat-mounted retinas were captured by fluorescent microscopy and quantitate by ImageJ program.

For H&E analysis, 10 μm sections were cut from frozen OCT blocks, mounted onto glass slides, fixed with 4% PFA, and washed with PBS and water. Hematoxylin (Vector Labs) was applied for 2 min, and bluing agent was added for 1 min. Slides were washed 3X with water, and 1x with 70% EtOH

for 5 min each. Eosin was add for 30sec, followed by 2x in 70% EtOH, 2x in 95%, EtOH, 2x in 100% EtOH (1-2 min each), and dipped into xylene for 2 min. Slides were mounted with Vectashield (Vector Labs), and analyzed with light microscopy.

Cell culture and reagents:

HUVEC were grown in Medium200 and Low Serum Growth Supplement (Cascade biologics/Gibco/Invitrogen). Neuroblastoma tumor cell lines (Kelly, IMR32, Lan-5, SK-N-BE2, SK-N-SH, SY5Y, SHEP) were obtained from the UCSF Cell Culture Facility. Human primary lines SFNB-05,06,07 were isolated from patients' neuroblastoma tumors, dissociated and cultured in N5 with 10% serum. SHEP-TET21/N were from Jason Shohet (Baylor University, Houston, TX). Stable SHEP N-MYC^{WT}, SHEP N-MYC^{T50A} were a gift from Dr. Anna Kenney, and previously described (*12*). Full length human $MYCN^{T58A}$ was generated in-house, from $MYCN^{WT}$ by site directed mutagenesis (Quickchange II kit) and cloned into pLenti6.3 lentiviral plasmid (Invitrogen). Multiclonal, stably transduced cell lines were produced by selection with blasticidin. Neuroblastoma cells were grown in RPMI, N5 or DMEM with 10% fetal bovine serum (FBS). In most experiments, cells were conditioned in 2% FBS for 5h and replaced with full media and recombinant human insulin-like growth factor-I (Invitrogen) at 20 ng/mL for 1h before harvesting. NVP-BEZ235 (Novartis) was reconstituted to 10M in DMSO for *in vitro* or PEG300 for *in vivo*.

Mission Lentiviral shRNA transduction particles (pLKO.1-puro) for human MYCN, HUWE1, and shRNA-control (non-targeting construct) (Sigma-Aldrich, MO) were used according to standard SIGMA lentiviral transduction protocol. Stable cell lines were selected with puromycin (2 µg/ml) for 48h.

Immunoblotting.

Lysates were collected, sonicated and cleared as described (*12*). Primary antibodies were: anti-MYCN, anti-VEGFA (Abcam), anti-Akt, anti- rpS6, anti-phosphorylated S473 Akt, [and] anti-rpS6 (Cell Signaling Technology), anti-Actin (Santa Cruz) and ß-tubulin (Upstate), anti-Huwe1 (Lifespan Biosciences), anti-Lasu1 (Bethyl Laboratories). Immunoblots were developed using horseradish peroxidase–conjugated secondary antibodies (Calbiochem) and Enhanced Chemiluminescence Plus reagents (Amersham).

Real-time PCR analysis

Total RNA isolation was collected with TRI Reagent kit (Ambion/ABI). qRT-PCR was done with ThermoScript RT-PCR System plus Platinum -*Taq* DNA Polymerase and *Power* SYBR® Green PCR Master Mix (Invitrogen), using standard methodology. Output readings were collected with ABI 7900HT system. DNA primers were:

Human MYCN, 5′CGACCACAAGGCCCTCAGTA-3′ (sense) and 5′CAGCCTTGGTG TTGGAGGAG-3′ (anti-sense),

Human VEGF, 5′-CCATGAACTTTCTGCTGTCTT-3′ (sense) and 5′-ATCGCATCAGGGGCACACAG-3′ (anti-sense)

Mouse VEGF, 5′-TACCTCCACCATGCCAAGTGGT-3′ (sense) and 5′-AGGACGGCTTGAAGATGTAC-3′ (anti-sense)

Control mouse β-actin, 5′-GACGGCCCAGTCATCACTAATG-3′ (sense) and 5′-TGCCA CAGGATCCATACCC-3′ (anti-sense).

Relative expression of MYCN and VEGF in the sample was normalized to the expression of an internal control (β-actin).

Boyden chamber migration assay

Cell migration was studied using Boyden chambers with 8μm pores (BD Biosciences). Transwell inserts were coated with Attachment Factor (Cascade/Invitrogen). Basal Medium 200 with FBS was used in all migration assays. First, neuroblastoma cells were resuspended in media, and $1*10^5$ cells (500 μL) plated in the bottom chamber, incubated for 3h, with NVP-BEZ235 or vehicle then added. After 16h, HUVEC ($1x10^5$ cells suspended in 100μL of assay media) were added to the upper chamber of transwell inserts. To control for spontaneous migration, HUVEC were also plated in the top chamber without neuroblastoma cells in the bottom. After 16h of co-incubation, non-migrated HUVEC in the upper surface of the membrane were scraped off. Cells migrating to the lower surface were then stained (SYTOX, Molecular Probes/ Invitrogen), and imaged at 5x. Quantification of 6 randomly selected fields per condition was performed using ImageJ program

(NIH), normalized to the internal control. All experiments were done in triplicate, and repeated at least three times.

Proliferation and viability assays

Neuroblastoma cells were suspended in basal RPMI , DMEM, or N5 with 1% FBS, and plated at 2000-3000 cells per well in 96-well tissue culture plates (Corning/Sigma Aldrich). Cells were incubated at 37°C for 16 hrs, and then changed into fresh media, containing NVP-BE235 (1 μM) or vehicle. To measure proliferation 24 hrs after plating, BrdU labeling solution from Cell Proliferation ELISA (Colorimetric Kit, Roche Bioscience) was added and cells incubated for another 24 hrs at 37°C. BrdU incorporation was determined by chemiluminescence immunoassay. To measure viable cells, DNA content was analyzed at 48hrs after plating using Cyquant NF assay kit (Invitrogen) according to the manufacturer's protocol. All experiments were repeated at least three times with 6 replicates.

VEGF ELISA

Neuroblastoma cells were split into 6 well plates and treated with vehicle or NVP-BEZ235 (1 μM). Media was harvested from cultures at 48h. Media was assayed for VEGF protein levels, and measured by Human VEGF QuantiGlo ELISA Kit (R&D Systems) and was determined by chemiluminescence immunoassay. All experiments were repeated at least three times with 6 replicates.

Statistical Analysis

GraphPad Prism program version 5.01 was used for Kaplan Meier and Log-Rank test (GraphPad Software, Inc.). JMP program versions 8 and 9 were used for Student's t-Test (SAS Corp). P value <0.05 indicates statistical significance.

REFERENCES

1. J. M. Maris, Recent advances in neuroblastoma. *N Engl J Med* **362**, 2202).

2. W. A. Weiss, K. Aldape, G. Mohapatra, B. G. Feuerstein, J. M. Bishop, Targeted expression of MYCN causes neuroblastoma in transgenic mice. *EMBO J* **16**, 2985 (1997).

3. C. S. Hackett, J. G. Hodgson, M. E. Law, J. Fridlyand, K. Osoegawa, P. J. de Jong, N. J. Nowak, D. Pinkel, D. G. Albertson, A. Jain, R. Jenkins, J. W. Gray, W. A. Weiss, Genome-wide array CGH analysis of murine neuroblastoma reveals distinct genomic aberrations which parallel those in human tumors. *Cancer Res* **63**, 5266 (2003).

4. D. Meitar, S. E. Crawford, A. W. Rademaker, S. L. Cohn, Tumor angiogenesis correlates with metastatic disease, N-myc amplification, and poor outcome in human neuroblastoma. *J Clin Oncol* **14**, 405 (1996).

5. T. A. Baudino, C. McKay, H. Pendeville-Samain, J. A. Nilsson, K. H. Maclean, E. L. White, A. C. Davis, J. N. Ihle, J. L. Cleveland, c-Myc is essential for vasculogenesis and angiogenesis during development and tumor progression. *Genes Dev* **16**, 2530 (2002).

6. R. H. Gold, Indications and risk-benefit of mammography. *J Fam Pract* **8**, 1135 (1979).

7. A. S. Chung, J. Lee, N. Ferrara, Targeting the tumour vasculature: insights from physiological angiogenesis. *Nat Rev Cancer* **10**, 505).

8. U. E. Knies-Bamforth, S. B. Fox, R. Poulsom, G. I. Evan, A. L. Harris, c-Myc interacts with hypoxia to induce angiogenesis in vivo by a vascular endothelial growth factor-dependent mechanism. *Cancer Res* **64**, 6563 (2004).

9. J. Kang, P. G. Rychahou, T. A. Ishola, J. M. Mourot, B. M. Evers, D. H. Chung, N-myc is a novel regulator of PI3K-mediated VEGF expression in neuroblastoma. *Oncogene* **27**, 3999 (2008).

10. A. Lasorella, G. Rothschild, Y. Yokota, R. G. Russell, A. Iavarone, Id2 mediates tumor initiation, proliferation, and angiogenesis in Rb mutant mice. *Mol Cell Biol* **25**, 3563 (2005).

11. A. M. Kenney, H. R. Widlund, D. H. Rowitch, Hedgehog and PI-3 kinase signaling converge on Nmyc1 to promote cell cycle progression in cerebellar neuronal precursors. *Development* **131**, 217 (2004).

12. L. Chesler, C. Schlieve, D. D. Goldenberg, A. Kenney, G. Kim, A. McMillan, K. K. Matthay, D. Rowitch, W. A. Weiss, Inhibition of phosphatidylinositol 3-kinase destabilizes MYCN protein and blocks malignant progression in neuroblastoma. *Cancer Res* **66**, 8139 (2006).

13. J. I. Johnsen, L. Segerstrom, A. Orrego, L. Elfman, M. Henriksson, B. Kagedal, S. Eksborg, B. Sveinbjornsson, P. Kogner, Inhibitors of

mammalian target of rapamycin downregulate MYCN protein expression and inhibit neuroblastoma growth in vitro and in vivo. *Oncogene* **27**, 2910 (2008).

14. H. P. Gerber, A. McMurtrey, J. Kowalski, M. Yan, B. A. Keyt, V. Dixit, N. Ferrara, Vascular endothelial growth factor regulates endothelial cell survival through the phosphatidylinositol 3'-kinase/Akt signal transduction pathway. Requirement for Flk-1/KDR activation. *J Biol Chem* **273**, 30336 (1998).

15. C. R. Schnell, F. Stauffer, P. R. Allegrini, T. O'Reilly, P. M. McSheehy, C. Dartois, M. Stumm, R. Cozens, A. Littlewood-Evans, C. Garcia-Echeverria, S. M. Maira, Effects of the dual phosphatidylinositol 3-kinase/mammalian target of rapamycin inhibitor NVP-BEZ235 on the tumor vasculature: implications for clinical imaging. *Cancer Res* **68**, 6598 (2008).

16. R. Sears, F. Nuckolls, E. Haura, Y. Taya, K. Tamai, J. R. Nevins, Multiple Ras-dependent phosphorylation pathways regulate Myc protein stability. *Genes Dev* **14**, 2501 (2000).

17. L. C. Cantley, The phosphoinositide 3-kinase pathway. *Science* **296**, 1655 (2002).

18. D. C. Cho, M. B. Cohen, D. J. Panka, M. Collins, M. Ghebremichael, M. B. Atkins, S. Signoretti, J. W. Mier, The efficacy of the novel dual PI3-kinase/mTOR inhibitor NVP-BEZ235 compared with rapamycin in renal cell carcinoma. *Clin Cancer Res* **16**, 3628).

19. S. M. Maira, F. Stauffer, J. Brueggen, P. Furet, C. Schnell, C. Fritsch, S. Brachmann, P. Chene, A. De Pover, K. Schoemaker, D. Fabbro, D. Gabriel, M. Simonen, L. Murphy, P. Finan, W. Sellers, C. Garcia-Echeverria, Identification and characterization of NVP-BEZ235, a new orally available dual phosphatidylinositol 3-kinase/mammalian target of rapamycin inhibitor with potent in vivo antitumor activity. *Mol Cancer Ther* (2008).

20. W. Lutz, M. Stohr, J. Schurmann, A. Wenzel, A. Lohr, M. Schwab, Conditional expression of N-myc in human neuroblastoma cells increases expression of alpha-prothymosin and ornithine decarboxylase and accelerates progression into S-phase early after mitogenic stimulation of quiescent cells. *Oncogene* **13**, 803 (1996).

21. X. Zhao, D. A. D, W. K. Lim, M. Brahmachary, M. S. Carro, T. Ludwig, C. C. Cardo, F. Guillemot, K. Aldape, A. Califano, A. Iavarone, A. Lasorella, The N-Myc-DLL3 cascade is suppressed by the ubiquitin ligase Huwe1 to inhibit proliferation and promote neurogenesis in the developing brain. *Dev Cell* **17**, 210 (2009).

22. X. Zhao, J. I. Heng, D. Guardavaccaro, R. Jiang, M. Pagano, F. Guillemot, A. Iavarone, A. Lasorella, The HECT-domain ubiquitin ligase Huwe1 controls neural differentiation and proliferation by destabilizing the N-Myc oncoprotein. *Nat Cell Biol* **10**, 643 (2008).

23. M. Yada, S. Hatakeyama, T. Kamura, M. Nishiyama, R. Tsunematsu, H. Imaki, N. Ishida, F. Okumura, K. Nakayama, K. I. Nakayama, Phosphorylation-dependent degradation of c-Myc is mediated by the F-box protein Fbw7. *EMBO J* **23**, 2116 (2004).

24. T. Otto, S. Horn, M. Brockmann, U. Eilers, L. Schuttrumpf, N. Popov, A. M. Kenney, J. H. Schulte, R. Beijersbergen, H. Christiansen, B. Berwanger, M. Eilers, Stabilization of N-Myc is a critical function of Aurora A in human neuroblastoma. *Cancer Cell* **15**, 67 (2009).

25. J. H. Mao, I. J. Kim, D. Wu, J. Climent, H. C. Kang, R. DelRosario, A. Balmain, FBXW7 targets mTOR for degradation and cooperates with PTEN in tumor suppression. *Science* **321**, 1499 (2008).

26. C. Schulein, M. Eilers, N. Popov, PI3K-dependent phosphorylation of Fbw7 modulates substrate degradation and activity. *FEBS Lett*).

27. A. L. Yu, A. L. Gilman, M. F. Ozkaynak, W. B. London, S. G. Kreissman, H. X. Chen, M. Smith, B. Anderson, J. G. Villablanca, K. K. Matthay, H. Shimada, S. A. Grupp, R. Seeger, C. P. Reynolds, A. Buxton, R. A. Reisfeld, S. D. Gillies, S. L. Cohn, J. M. Maris, P. M. Sondel, Anti-GD2 antibody with GM-CSF, interleukin-2, and isotretinoin for neuroblastoma. *N Engl J Med* **363**, 1324).

28. H. Cui, T. Li, H. F. Ding, Linking of N-Myc to death receptor machinery in neuroblastoma cells. *J Biol Chem* **280**, 9474 (2005).

29. S. Fulda, W. Lutz, M. Schwab, K. M. Debatin, MycN sensitizes neuroblastoma cells for drug-induced apoptosis. *Oncogene* **18**, 1479 (1999).

30. A. Bender, D. Opel, I. Naumann, R. Kappler, L. Friedman, D. von Schweinitz, K. M. Debatin, S. Fulda, PI3K inhibitors prime neuroblastoma cells for chemotherapy by shifting the balance towards pro-apoptotic Bcl-2 proteins and enhanced mitochondrial apoptosis. *Oncogene* **30**, 494).

31. T. Teitz, J. J. Stanke, S. Federico, C. L. Bradley, R. Brennan, J. Zhang, M. D. Johnson, J. Sedlacik, M. Inoue, Z. M. Zhang, S. Frase, J. E. Rehg, C. M. Hillenbrand, D. Finkelstein, C. Calabrese, M. A. Dyer, J. M. Lahti, Preclinical models for neuroblastoma: establishing a baseline for treatment. *PLoS One* **6**, e19133).

32. H. Komuro, S. Kaneko, M. Kaneko, Y. Nakanishi, Expression of angiogenic factors and tumor progression in human neuroblastoma. *J Cancer Res Clin Oncol* **127**, 739 (2001).

33. G. Qing, N. Skuli, P. A. Mayes, B. Pawel, D. Martinez, J. M. Maris, M. C. Simon, Combinatorial regulation of neuroblastoma tumor progression by N-Myc and hypoxia inducible factor HIF-1alpha. *Cancer Res* **70**, 10351).

34. J. W. Kim, P. Gao, Y. C. Liu, G. L. Semenza, C. V. Dang, Hypoxia-inducible factor 1 and dysregulated c-Myc cooperatively induce vascular endothelial growth factor and metabolic switches hexokinase

2 and pyruvate dehydrogenase kinase 1. *Mol Cell Biol* **27**, 7381 (2007).

35. N. M. Sodir, L. B. Swigart, A. N. Karnezis, D. Hanahan, G. I. Evan, L. Soucek, Endogenous Myc maintains the tumor microenvironment. *Genes Dev* **25**, 907).

Figure 2-1. *MYCN*-amplification is a biomarker for sensitivity to PI3K/mTOR inhibition

(**A**) Viability screen: *MYCN*-amplified cells (human primary culture SFNB-06, and three cell lines: IMR32, Lan-5, SK-N-BE2 I) were sensitive to NVP-BEZ235 as compared with non-amplified cells (two human primary cultures SFNB-05, 07; and cell lines: SK-N-SH, SY5Y, SHEP). *P<0.05 by Student's t-test.

(**B**) Proliferation screen: NVP-BEZ235 showed improved efficacy in blocking *MYCN*-amplified cells as compared with non-amplified, *P<0.05 by Student's t-test.

Figure 2-1

A

Viability Screen

B

Proliferation Screen
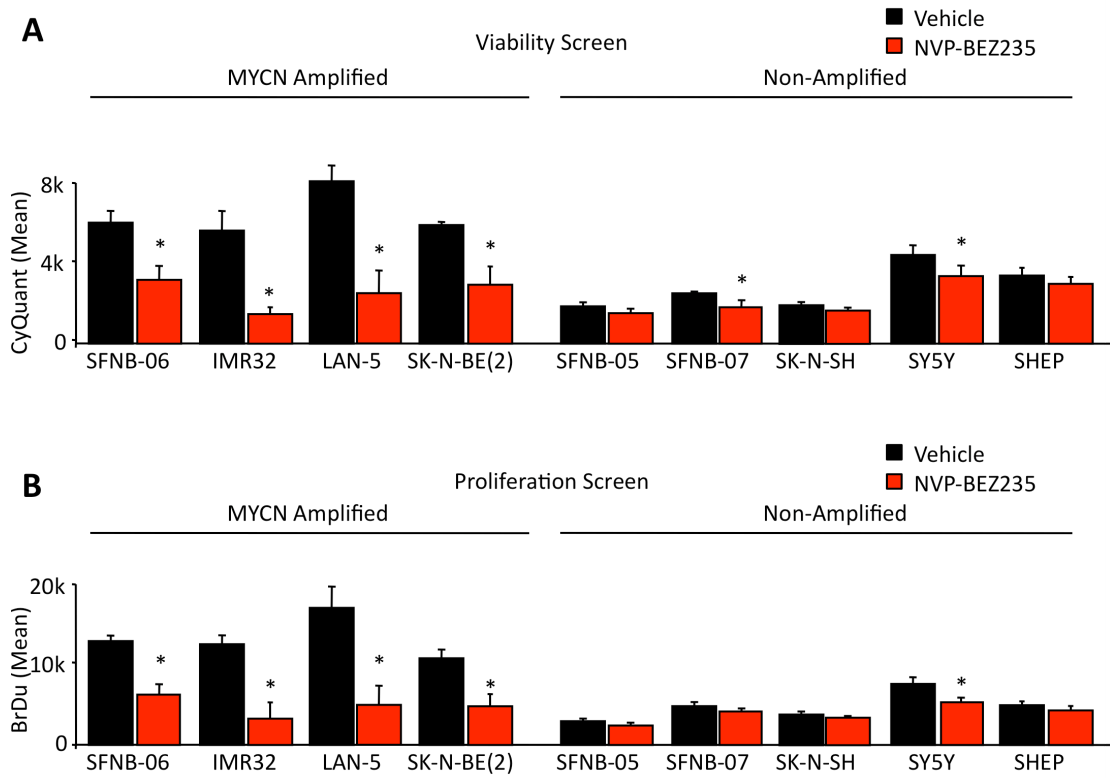
Figure 2-2. A dual PI3K/mTOR inhibitor improves survival in GEM and primary orthtopic xenograft models of MYCN-driven neuroblastoma

(**A**) Tumor-bearing TH-*MYCN* mice were treated with NVP-BEZ235 (35mg/kg) or PEG-300 vehicle once daily by oral gavage, for 28d. Kaplan-Meyer analysis demonstrates that NVP-BEZ235 enhanced mice survival (n=5 for each group, P<0.003 by Log-Rank Test). Arrow indicates cessation of therapy at 28d.

(**B**) A heavily pretreated primary *MYC*N amplified human tumor (SFNB-06) was established orthotopically, and mice treated with NVP-BEZ235 or vehicle as above, for 28d. NVP-BEZ235 prolonged survival (n=10 for each group, P<0.049 by Log-Rank Test). Arrow again indicates cessation of therapy at 28d (arrow).

Figure 2-2

A TH-*MYCN* Survival Study
  — · — Vehicle
  ——— NVP-BEZ235

% Survival

n=5   n=5

Days   0   10   20   30   40   50

p<0.003

B SFNB-06 Survival Study
  — · — Vehicle
  — — — NVP-BEZ235

% Survival

n=10

n=10

Days   0   20   40   60   80   100

p<0.049
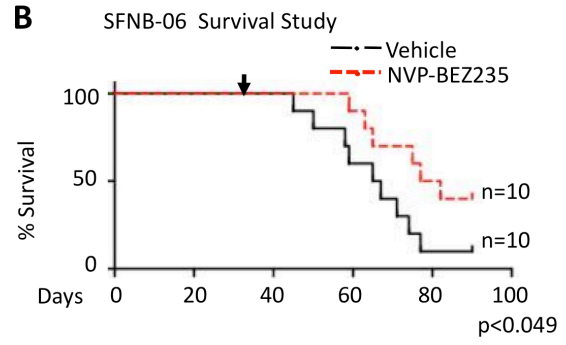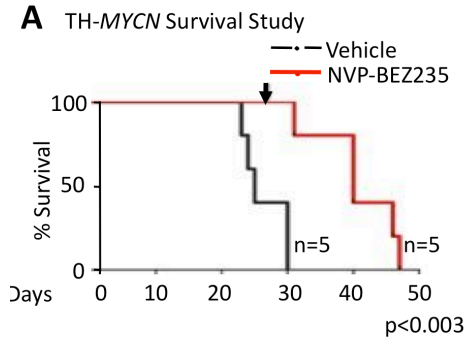
Figure 2-3. A dual PI3K/mTOR inhibitor inhibits tumor growth, and reduces tumor burden

(**A,** tumor-bearing TH-*MYCN* mice were treated with NVP-BEZ235 (35mg/kg) or PEG-300 vehicle once daily by oral gavage for 14d. NVP-BEZ235 treatment led to decreased tumor volume and weight.

(**B**) orthotopic xenografts of SFNB-06 with tumors were treated with NVP-BEZ235 (35mg/kg) or PEG-300 vehicle. NVP-BEZ235 treatment also led to decreased tumor burden in this model (*,P<0.05, Student's t-test).

Figure 2-3

A

TH-*MYCN* tumor burden

B

SFNB-06 tumor burden
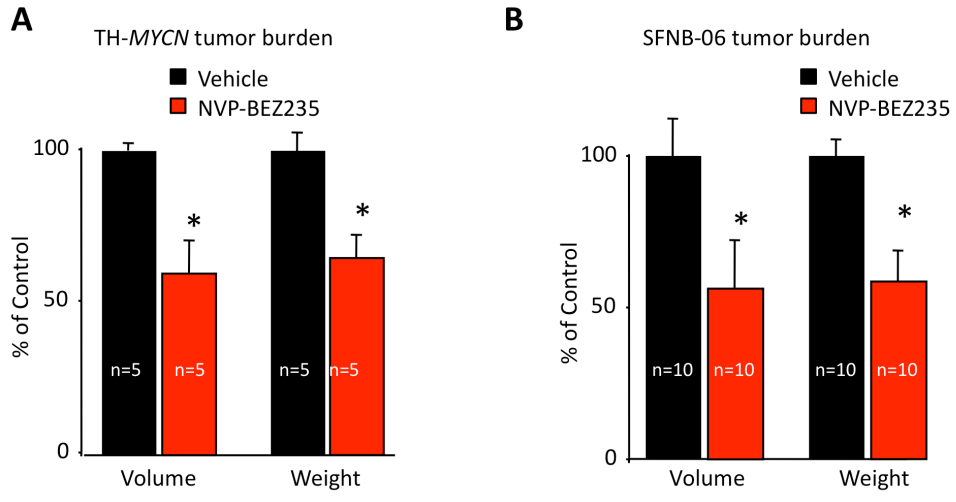
Figure 2-4. NVP-BEZ235 suppresses both proliferation of tumor cells, and angiogenesis in GEM neuroblastoma model.

(**A-H**) Tumors from mice transgenic for TH-*MYCN* were treated with NVP-BEZ235 (35mg/kg) or PEG-300 vehicle once daily by oral gavage, and mice were sacrificed at 14d of treatment. Endothelial cell density (CD31), pericyte density (α-SMA), proliferation of tumor cells (Ki67), and H&E staining were assessed. Scale bars = 50 μm. N=3 for each arm.

(**I**) Quantitations of (**A-C, E-G**) using imageJ (*P<0.0008, Student's t-test)

In all quantitations, vehicle arms were normalized to 100%; NVP-BEZ235 arms were graphed as percent of vehicle.

Figure 2-4
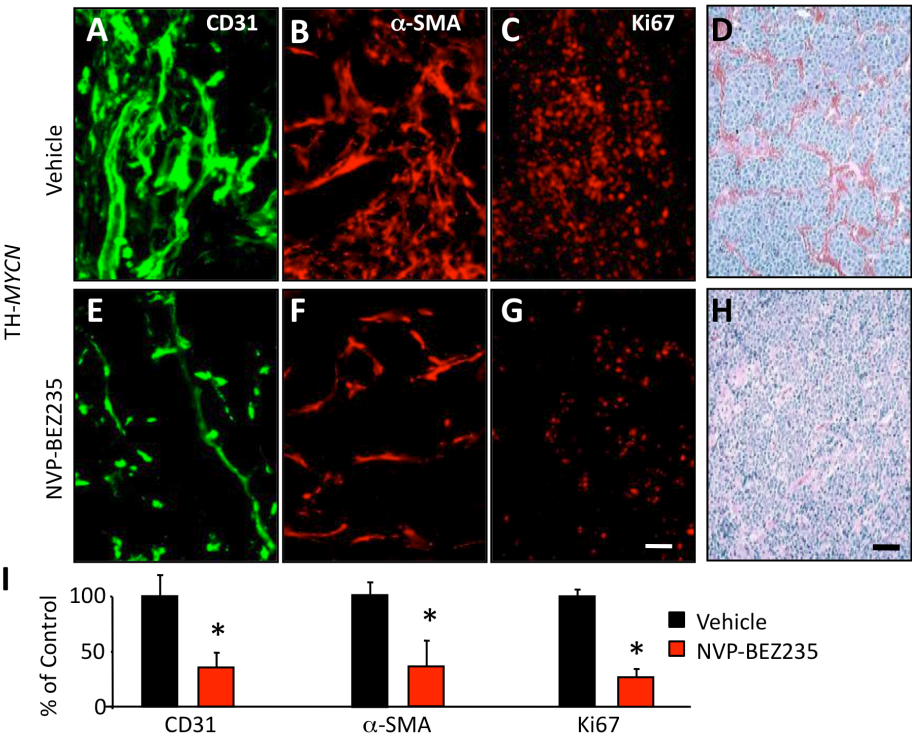
Figure 2-5. A dual PI3K/mTOR inhibitor suppresses tumor progression and angiogenesis of *MYCN*-amplified human orthotopic xenograft model.

(**A-H**) Mice carrying *MYCN*-amplified human orthotopic xenografts (SFNB-06) were treated with NVP-BEZ235 or vehicle for 14d, collected, and analyzed as in (**A-I**).

(**I**) Quantitations of (**A-C, E-H**) with imageJ (*P< 0.0008, Student's t-test). N=3 for each arm.

In all quantitations, vehicle arms were normalized to 100%; NVP-BEZ235 arms were graphed as percent of vehicle

Figure 2-5
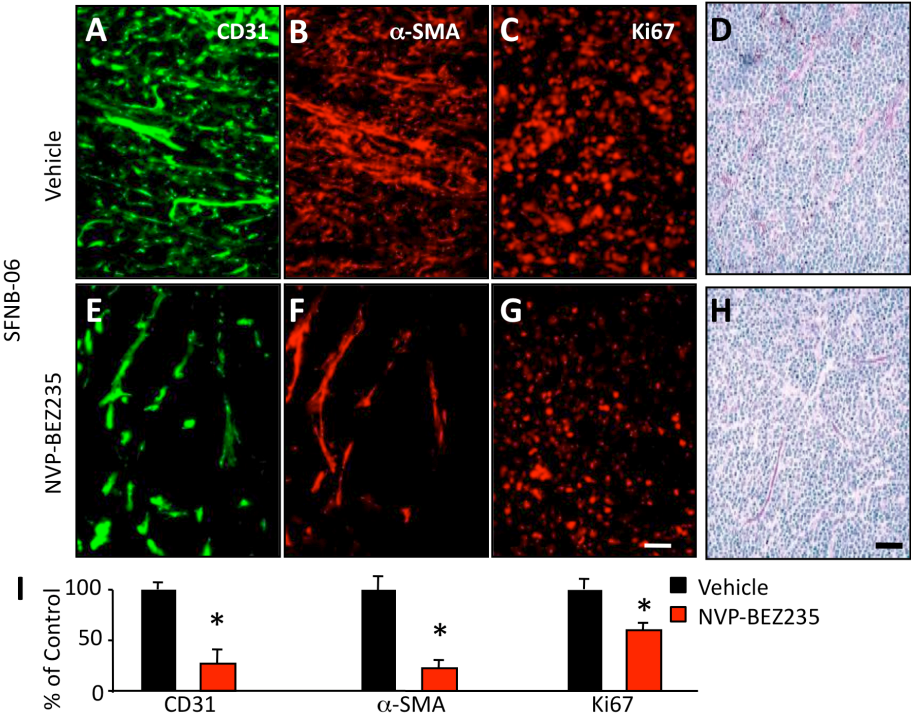
Figure 2-6. NVP-BEZ235 has little effect on normal vasculature.

(**A**) Vehicle and NVP-BEZ235 treated mice (35 mg/kg/d, 14d, by daily oral gavage) showed no significant difference in retinal vascular density (P=0.09). N=3 mice each arm.

(**B**) Quantitations of (**A**) Three representative images per mouse were quantitated using imageJ. Scale bar= 200 mm

Figure 2-6

A

Retinal study

Vehicle   NVP-BEZ235

B

■ Vehicle
■ NVP-BEZ235

Vascular Density
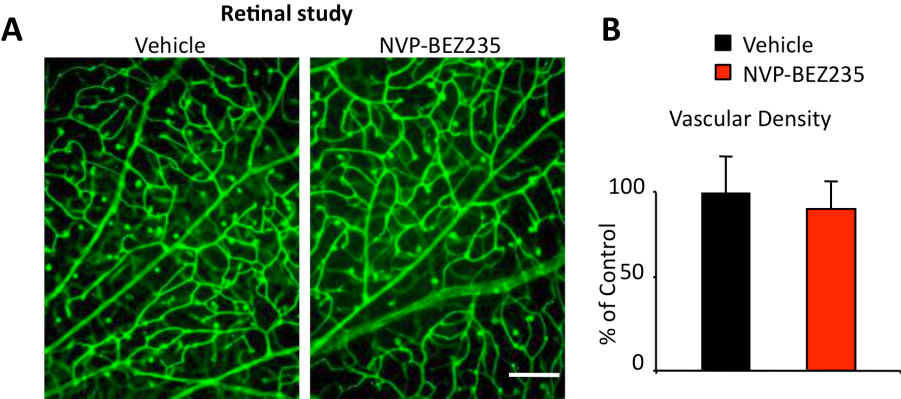
Figure 2-7. Cessation of NVP-BEZ235 allows tumor to relapse.

(**A-E**) Discontinuation of NVP-BEZ235 after 28d of treatment allowed tumor vessels (marked with CD31) and tumor cells (marked with Ki67) to grow back and proliferate robustly (as compared to Figure 2-4 **A-I**). Tumors from mice in the NVP-BEZ235 treatment arm were collected at the time of sacrifice and assessed by IHC. Scale bar=100 mm

Figure 2-7
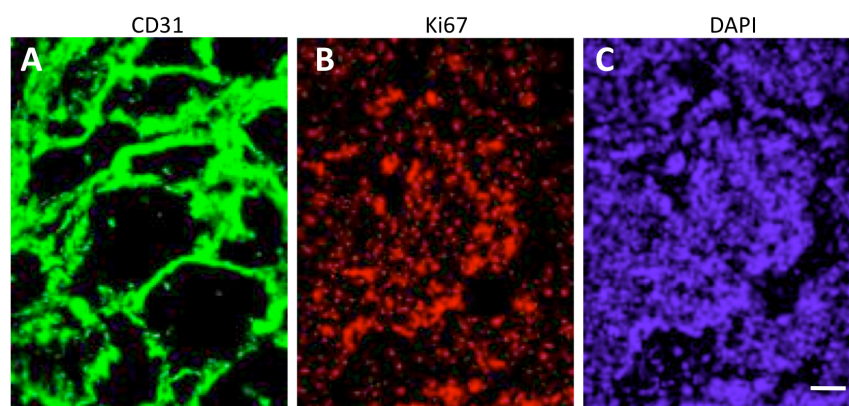
Relapse Tumors (14d after last NVP-BEZ235 treatment)

Figure 2-8. NVP-BEZ235 blocks PI3K/mTOR and destabilizes MYCN in vivo.

(**A**) Tumor bearing mice transgenic for TH-*MYCN* were treated daily with NVP-BEZ235 or vehicle for 7d or 14dWestern analysis demonstrates decreased levels of MYCN protein in tumor lysates from animals treated with NVP-BEZ235 in comparison with control.

(**B**) Western analysis of lysates from human orthotopic tumors confirms expression of MYCN in primary tumors and in vehicle treated orthotopic xenografts, with decreased levels of MYCN protein in lysates from 2 different xenografts, treated with NVP-BEZ235 for 14d.

Figure 2-8

A   TH-*MYCN*

Vehicle
NVP-BEZ235 (7d)
NVP-BEZ235 (14d)

MYCN
pAkt
Akt
prpS6
rpS6
Actin

B   SFNB-06

Original
Vehicle
NVP-BEZ235 (1)
NVP-BEZ235 (2)

MYCN
pAkt
Akt
prpS6
rpS6
β-tubulin
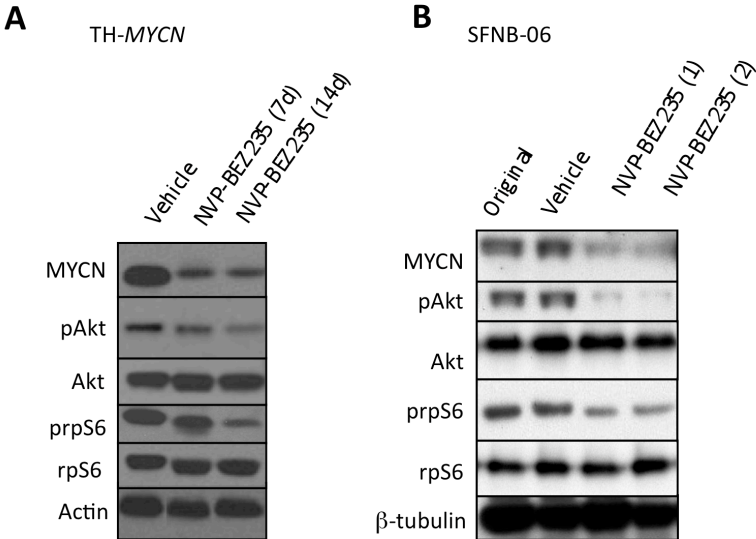
Figure 2-9. NVP-BEZ235 has little effect on MYCN mRNA level.

(**A,B**) Quantitative real-time RT-PCR demonstrating that NVP-BEZ235 (14d) had no significant effect on levels of MYCN mRNA in both the TH-*MYCN* and primary human SFNB-06 tumors P=0.75, P=0.62 by Student's t-test. Vehicle arms were normalized to 100%. NVP-BEZ235 arms were graphed as percent of vehicle

Figure 2-9

A

MYCN qRT-PCR
TH-*MYCN*

■ Vehicle
■ NVP-BEZ235

B

MYCN qRT-PCR
SFNB-06

■ Vehicle
■ NVP-BEZ235
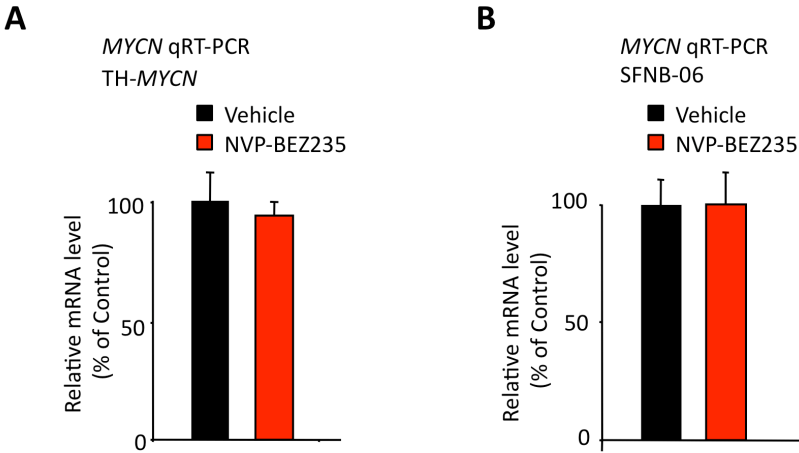
Figure 2-10. *MYCN* non-amplified cells with pLenti6.3 lentiviral control vector

(GFP tag) response similarly to NVP-BEZ235 as parental cells

SHEP cells transduced with pLenti6.3 lentiviral control vector (GFP tag) for

$MYCN^{WT}$ or $MYCN^{T58A}$ constructs.

Viability assay: SHEP vector-GFP control cell lines responsed to NVP-

BEZ235 similar to that observed in parental SHEP cells.

Figure 2-10

SHEP Vector-GFP control
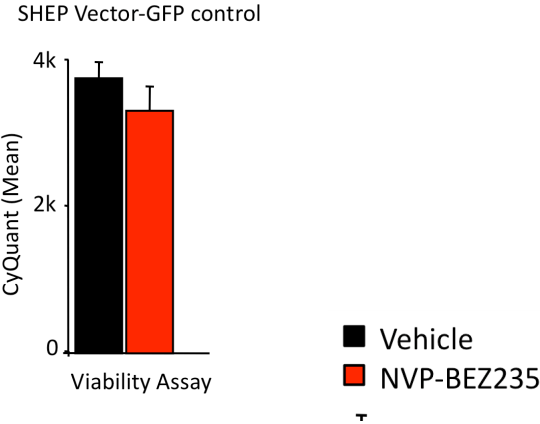
Figure 2-11. *MYCN^T58A* prolongs MYCN protein half-life.

(**A**) Cycloheximide pulse chase assay: CHX (50ug/ml) with vehicle, were added to *MYCN^WT* or *MYCN^T58A* cells over a 0-6h time course. *MYCN^T58A* protein showed a prolonged half-life.

(**B**) Cycloheximide pulse chase assay: CHX (50ug/ml) with NVP-BEZ235, were treated similar to A. MYCN^T58A protein showed a prolonged half-life, even in the presence of NVP-BEZ235.

Figure 2-11
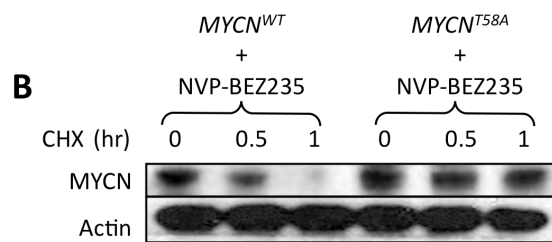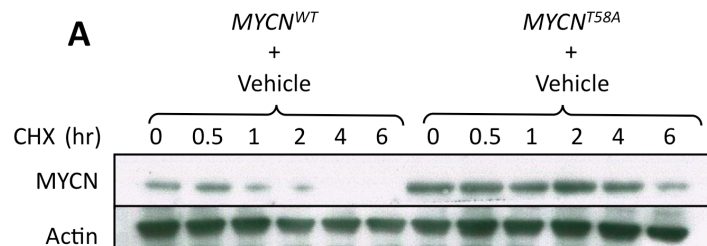
Figure 2-12. While inhibiting PI3K/mTOR pathway, NVP-BEZ235 has little effect on $MYCN^{T58A}$ protein level.

Western blot: $MYCN^{WT}$ *and* $MYCN^{T58A}$ cells were treated with vehicle or NVP-BEZ235 for 48h and collected for western blot. NVP-BEZ235 inhibits pAkt and prpS6 in both cell $MYCN^{WT}$ and $MYCN^{T58A}$ lines. However, $MYCN^{T58A}$ protein was resistant to NVP-BEZ235 as compared to $MYCN^{WT}$.

Figure 2-12
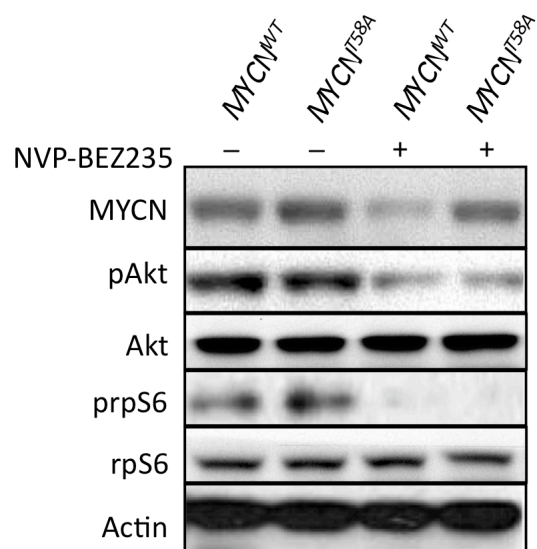
Figure 2-13. $MYCN^{T58A}$ cells conferred resistance to NVP-BEZ235

Proliferation and viability assays: $MYCN^{WT}$ and $MYCN^{T58A}$ cells were treated with vehicle or NVP-BEZ235 for 48h. Proliferation (BrDU) and viability (WST) of these cells are examined. Vehicle treated $MYCN^{WT}$ and $MYCN^{T58A}$ were normalized to 100%. NVP-BEZ treated arms were graphed as percent change of vehicle. $MYCN^{T58A}$ cells are more resistant to NVP-BEZ235 as compared to $MYCN^{WT}$ (*P<0.026, **P<0.05).

Figure 2-13
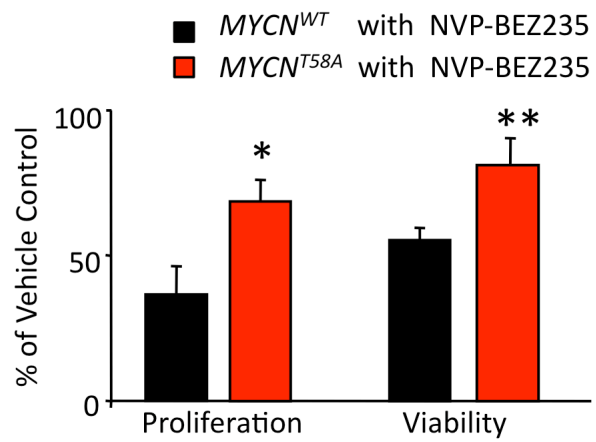
Figure 2-14. *MYCN* non-amplified cells induced minimal endothelial cell migration.

SHEP cells transduced with pLenti6.3 lentiviral control vector (GFP tag) for *MYCN^WT^* or *MYCN^T58A^* constructs.

Boyden chamber HUVEC migration assay: SHEP vector-GFP control induced very minimal migration (800 cell counts) as compared to *MYCN^WT^* or *MYCN^T58A^* cells (3000-4000 cell counts in Fig.1-15).
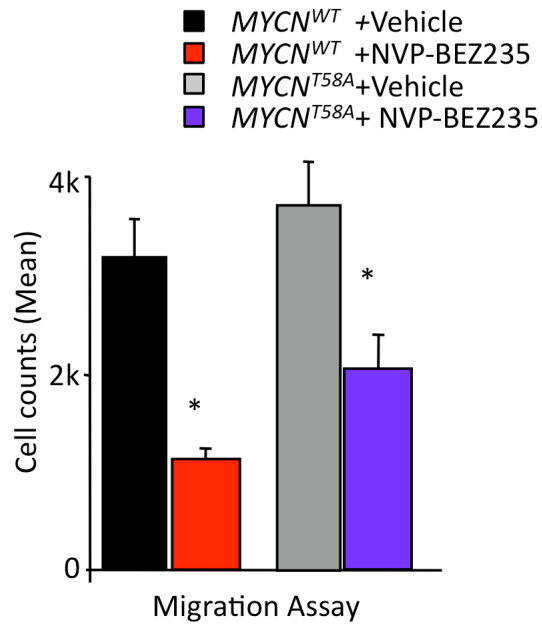
Figure 2-14

SHEP Vector-GFP control
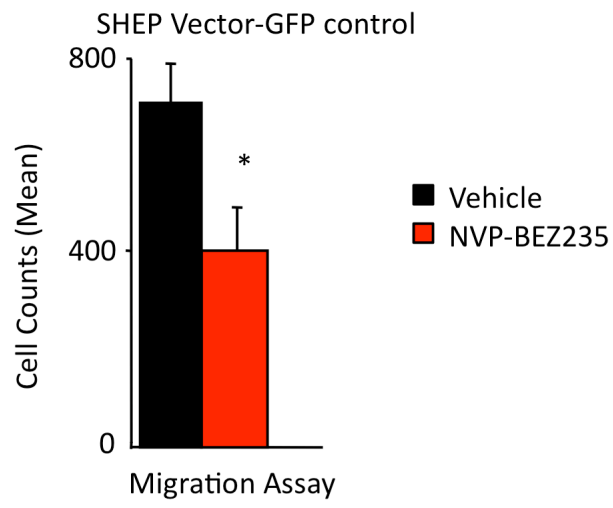
Migration Assay

Figure 2-15. MYCN protein stability is essential for induction of endothelial

cell migration and angiogenesis.

SHEP cells were stably transduced with *MYCN^{WT}* or *MYCN^{T58A}*.

HUVEC migration: HUVEC (upper chamber) with *MYCN^{WT}* or *MYCN^{T58A}* cells

(bottom chamber). NVP-BEZ235 reduced migration was blunted in *MYCN^{T58A}*

co-cultures(****P<0.008).

Figure 2-15

Legend (inside figure):
- $MYCN^{WT}$ +Vehicle
- $MYCN^{WT}$ +NVP-BEZ235
- $MYCN^{T58A}$+Vehicle
- $MYCN^{T58A}$+ NVP-BEZ235

Y-axis: Cell counts (Mean) — 4k, 2k, 0

X-axis: Migration Assay

Figure 2-16. MYCN drives paracrine signaling between tumor-vascular cells by inducing VEGFA.

Vehicle treated $MYCN^{WT}$ and $MYCN^{T58A}$ were normalized to 100%. NVP-BEZ treated arms were graphed as percent change of vehicle

(**A**) VEGF ELISA: NVP-BEZ235 suppressed levels of VEGF in $MYCN^{WT}$ cells, with blunting response in $MYCN^{T58A}$ cells (***P<0.002).

(**B**) Quantitative RT-PCR for VEGF: In response to NVP-BEZ235, levels of VEGF mRNA were significantly higher in $MYCN^{T58A}$ cells as compared with $MYCN^{WT}$, (*P< 0.001 by Student's t-test).

Figure 2-16

■ *MYCN^{WT}* with NVP-BEZ235
■ *MYCN^{T58A}* with NVP-BEZ235

A VEGF ELISA

B VEGF qRT-PCR
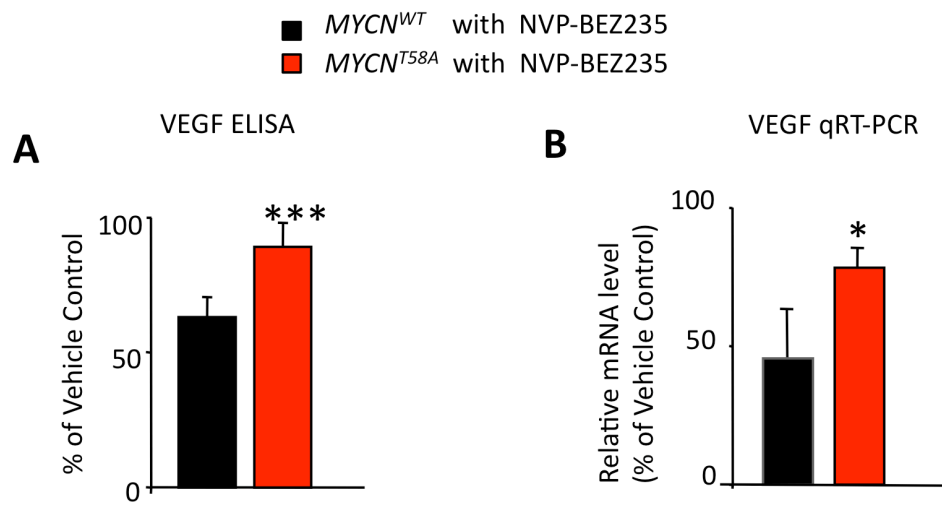
Figure 2-17. MYCN does not affect VEGFA protein stability.

CHX pulse chase assay: Stability of VEGFA protein (with control or NVP-BEZ235 treatment) is unaltered in SHEP Vector-GFP control, *MYCN^{WT}*, *MYCN^{T58A}*. This suggests that MYCN regulate VEGFA at the level of transcription.
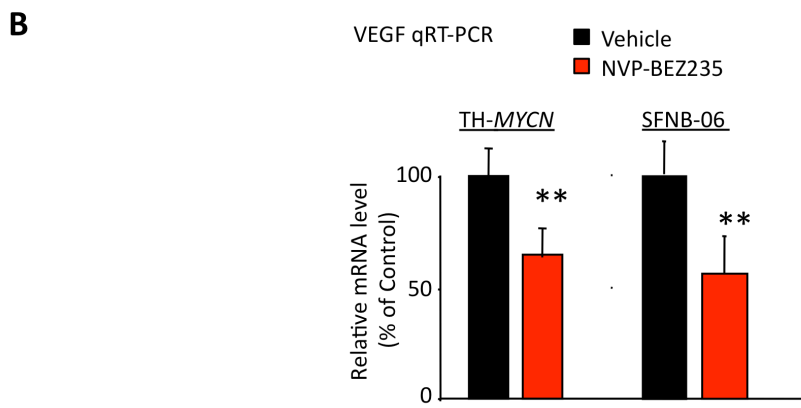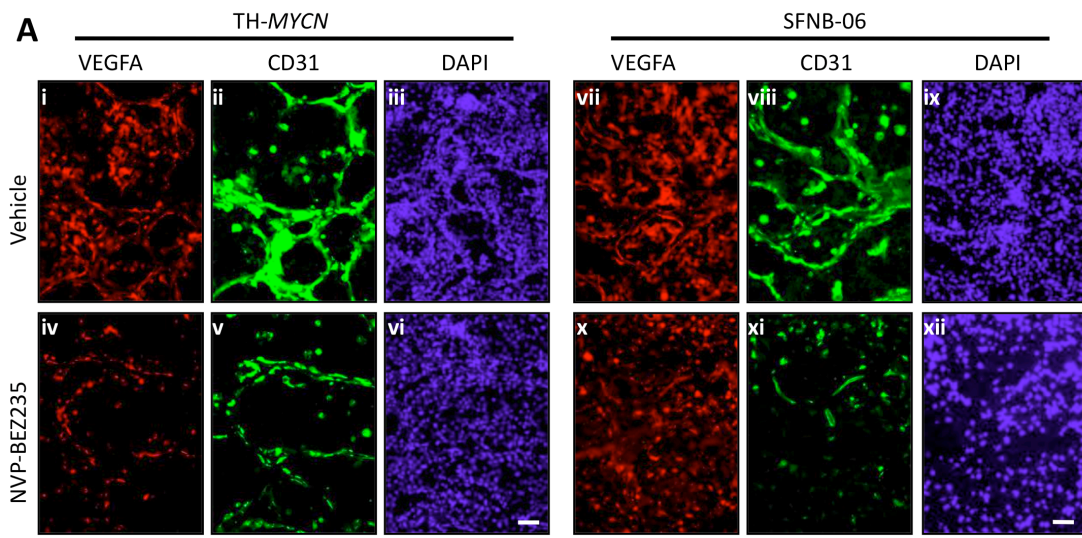
Figure 2-17
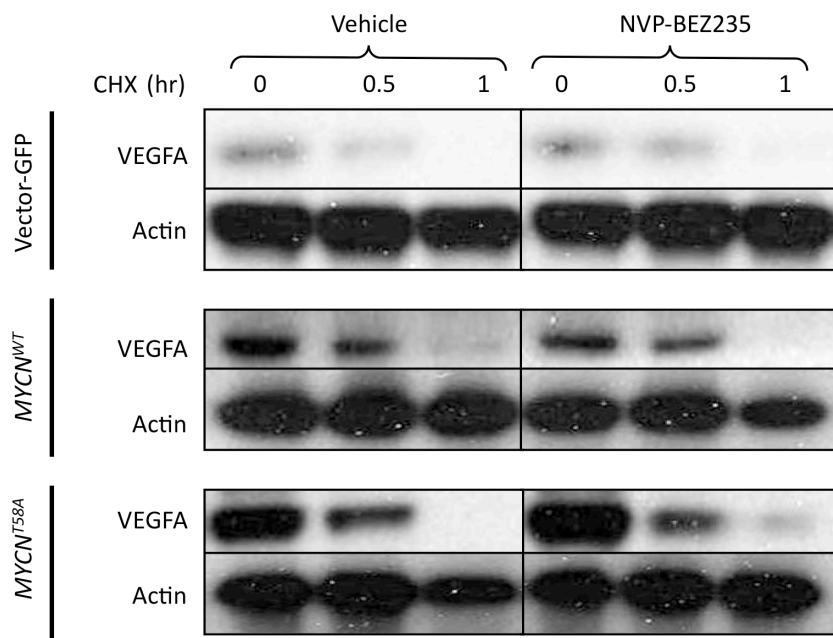
Figure 2-18. VEGFA levels correlated with expression of MYCN in vivo.

(**A**) IHC for VEGFA and vasculature: tumors from TH-*MYCN* and SFNB-06 (from Fig.1-4 and 1-5) showed that NVP-BEZ235 also affected expression of VEGFA. Scale bars = 50 μm. N=3 for each arm.

(**B**) Quantitative RT-PCR for VEGFA in tumors from TH-*MYCN* and SFNB-06 (shown in A) indicates significant reduction in VEGF mRNA in response to NVP-BEZ235, as compared with vehicle (**P< 0.0003 by Student's t-test).
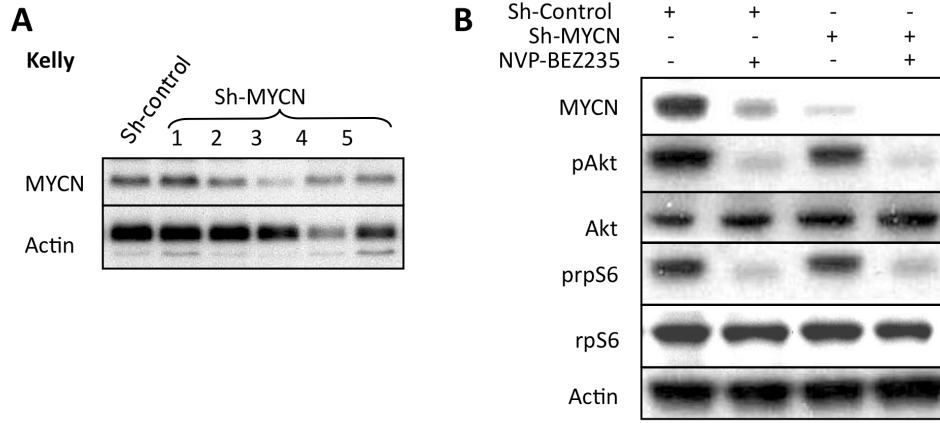
Figure 2-18

A

B

VEGF qRT-PCR

Figure 2-19. Knockdown of MYCN in *MYCN*-amplified neuroblastoma cells.

(**A**) *MYCN*-amplified Kelly cells were stably transduced with shRNA-MYCN, shRNA-control vector.

(**B**) Western Blot: sh-MYCN (#3) was as efficient as NVP-BEZ235 in suppressing MYCN, without altering p-Akt/p-rpS6.

Figure 2-19

A

Kelly

B

Sh-Control	+	+	-	-
Sh-MYCN	-	-	+	+
NVP-BEZ235	-	+	-	+

79

**Figure 2-20.** Knockdown of MYCN substantiates a role in paracrine signaling

(**A**)Proliferation and viability: sh-MYCN recapitulated the effects of NVP-BEZ235 (sh-MYCN vs. shRNA vehicle: *P<0.001, **P<0.007; sh-MYCN vs. NVP-BEZ235, #P<0.04).

(**B**) VEGF ELISA: sh-MYCN and NVP-BEZ235 similarly reduced VEGF (sh-MYCN vs. shRNA control,***P<0.005; sh-MYCN vs. NVP-BEZ235, ##P<0.04). HUVEC migration: sh-MYCN and NVP-BEZ235 blocked migration (sh-MYCN vs. shRNA control, ****, P<0.002; sh-MYCN + NVP-BEZ235 vs. sh-Control + vehicle, +P<0.0001).

(**C**) Quantitative RT-PCR for VEGFA mRNA: Knockdown of MYCN was as effective as NVP-BEZ235 (*P<0.03, Student's t-test). Combined knockdown of MYCN together with NVP-BEZ235 treatment significantly reduced VEGF mRNA, when compared with vehicle (+, P< 0.0001, Student's t-test).

In all quantifications, vehicle arms were normalized to 100% and NVP-BEZ235 arms were graphed as percent of vehicle.
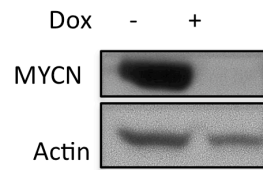
Figure 2-20
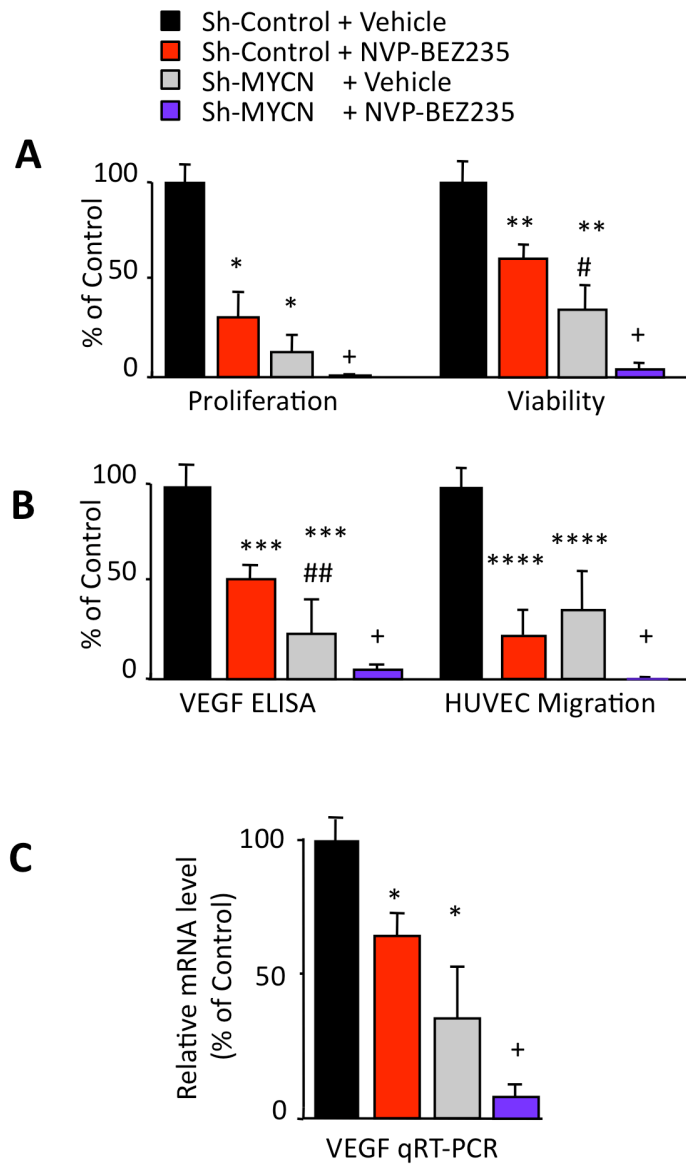
Figure 2-21. A doxycycline-inducible allele of MYCN

SHEP-TET21/N cells (*20*) were treated with dox (10 mg/ml) and/or NVP-BEZ235 for 48h.
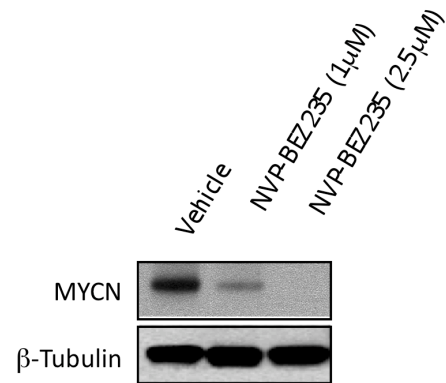
(**A, B**) WB: both dox and NVP-BEZ235 led to decreased levels of MYCN protein.

Figure 2-21

A

Dox   -   +

MYCN

Actin

B

MYCN

β-Tubulin

Vehicle

NVP-BEZ235 (1µM)

NVP-BEZ235 (2.5µM)

Figure 2-22. A role for MYCN in recruitment of endothelial cells.

SHEP-TET21/N cells (*20*) were treated with dox and/or NVP-BEZ235 for 48h as above.

(**A**) Proliferation and viability: dox (MYCN "off") and NVP-BEZ235 led to significant reduction in tumor cells vs. no dox (MYCN "on") or vehicle controls (*, **, $P< 0.001$). In viability assays, NVP-BEZ235 treated MYCN "off" conditions significantly reduced viability as compared to NVP-BEZ235 treated MYCN "on" conditions ([+]$P<0.02$). In all assays, combining MYCN "off" together with NVP-BEZ235 led to significant differences vs. MYCN "on" controls ([#]$P< 0.05$). NVP-BEZ235 treated MYCN "off" conditions were not significantly better than NVP-BEZ235 treated MYCN "on" conditions, $P>0.06$

VEGF ELISA**:** Suppression of MYCN by dox or NVP-BEZ235 resulted in decreased secretion of VEGF vs control (***$P< 0.009$).

HUVEC migration: TET21/N cells (lower chamber) with HUVEC (upper chamber). HUVECs responded similarly when co-cultured with vehicle treated MYCN "off" cells or with NVP-BEZ235 treated MYCN "on" cells, resulting in significant reduction in migration vs. vehicle MYCN "on" controls (****$P< 0.008$).

 (**B**) HUVEC Viability: dox treatment (10 mg/ml) did not significantly affect viability of HUVEC ($P=0.12$)
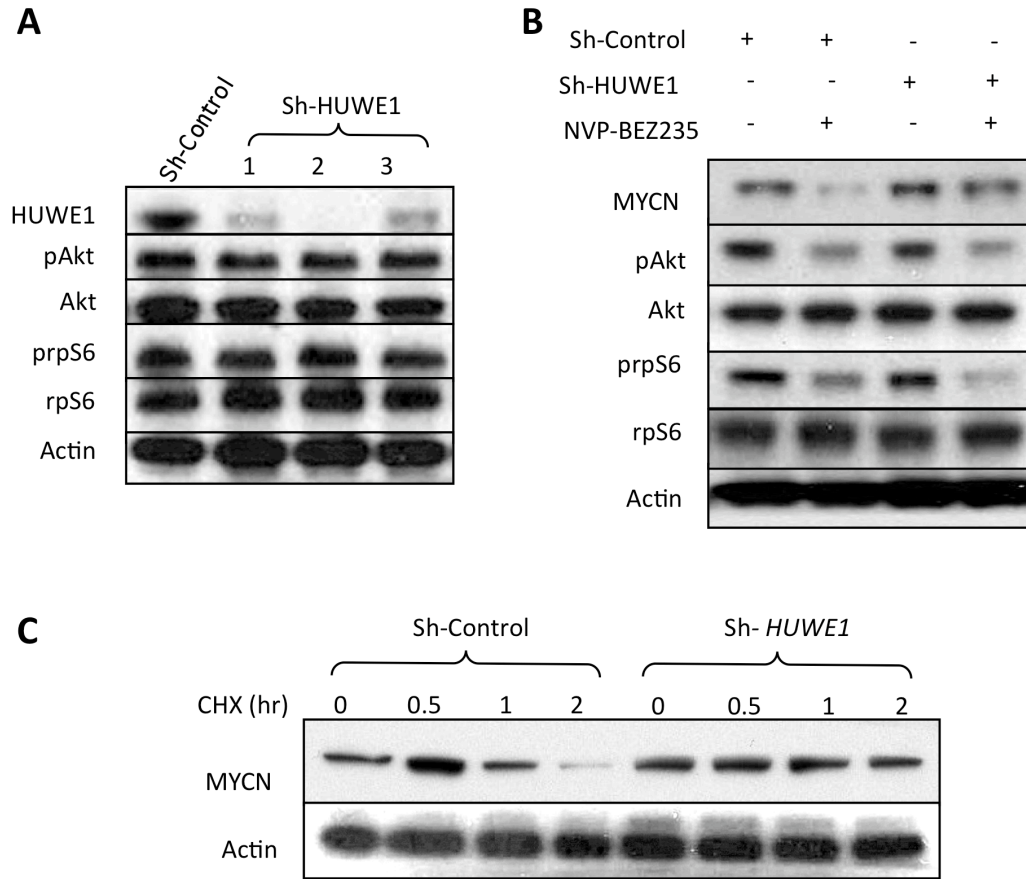
Figure 2-22
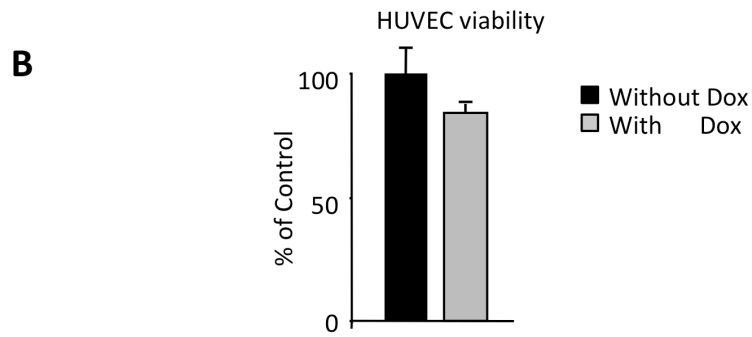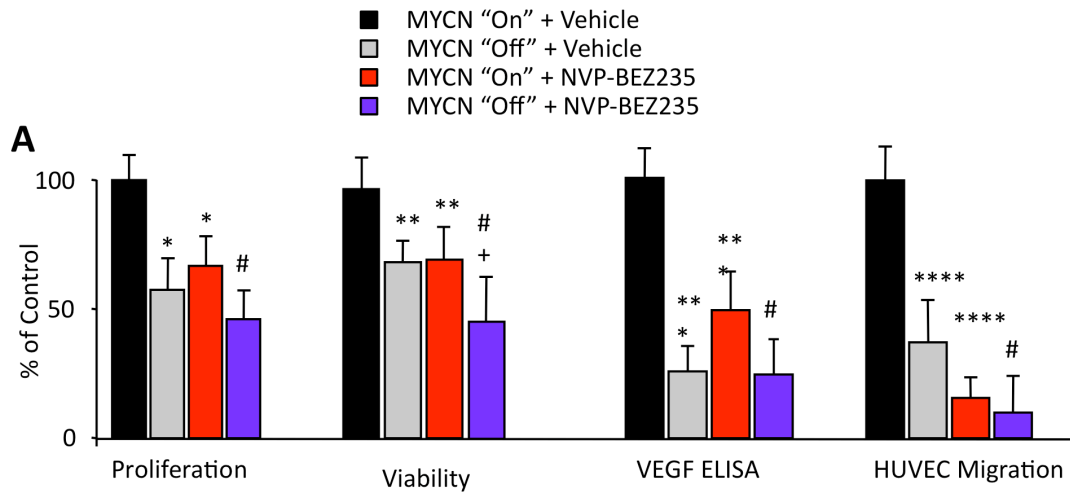
Figure 2-23. Impaired ubiquitination stabilizes MYCN protein

(**A**) Kelly *MYCN*-amplified neuroblastoma cells were stably transduced with 3 different HUWE1 shRNAs or shRNA control. Western analysis demonstrates that shRNA in lane-2(sh-1) knocked down HUWE1 without significantly affecting the PI3K target pAkt or mTOR target p-rpS6. Sh-1 was used for subsequent experiments.

(**B**) WB: HUWE1 knockdown promoted partial resistance to NVP-BEZ235 (lane 4 vs. 2 respectively).

(**C**) Cycloheximide pulse chase assay: CHX was added over a 2h time course. HUWE1 knockdown promoted longer half-life of MYCN vs. control.

Figure 2-23

A

B

Sh-Control	+	+	-	-
Sh-HUWE1	-	-	+	+
NVP-BEZ235	-	+	-	+

C

**Figure 2-24** HUWE1 knockdown reduces the efficacy of NVP-BEZ235.

Vehicle treated arms from both sh-control and HUWE1 knock-down lines were normalized to 100%, and NVP-BEZ treated arms were graphed as percent change compared to vehicle treated

Proliferation and viability assay: with NVP-BEZ235, HUWE1 knockdown cells were resistant to vs. sh-control cells (*,** P<0.003).

VEGF ELISA: NVP-BEZ235 blocks VEGF in sh-control, with significant resistance mediated by HUWE1 knockdown, (***, P<0.03).

HUVEC migration assay: HUWE1 or sh-control cells (lower chamber) with HUVEC (upper chamber). With NVP-BEZ235 treatment, HUWE1 knockdown cells were significantly resistant vs. sh-control cells (****, P< 0.003).
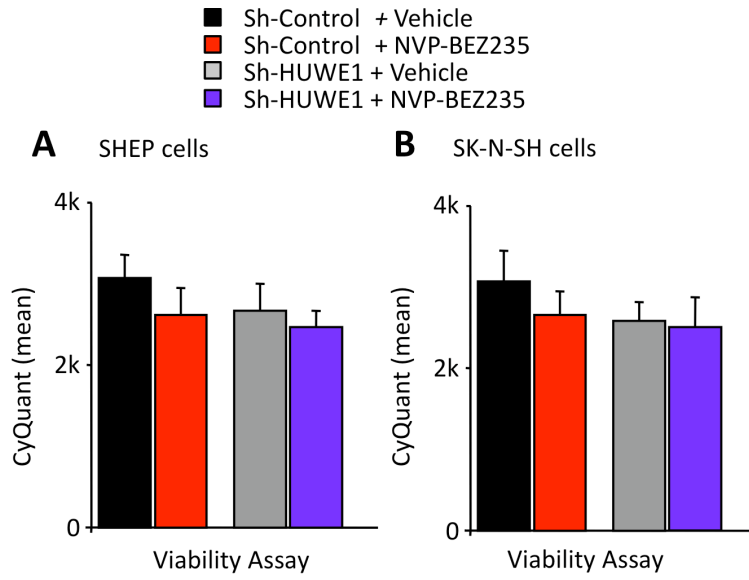
Figure 2-24
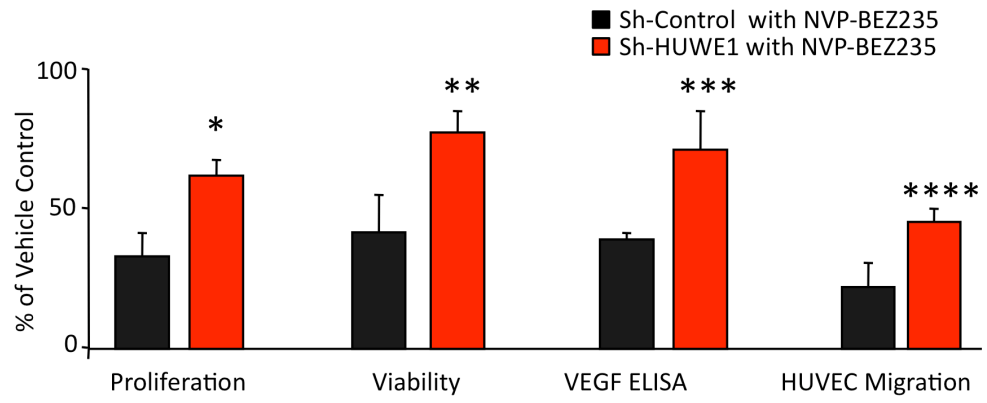
Figure 2-25 Minimal effect of HUWE1 knockdown in MYCN non-amplified neuroblastoma.

(**A,B**) Viability screens: non-amplified neuroblastoma cells (SHEP in **A**, and SK-N-SH in **B**) were transduced with sh-HUWE1. HUWE1 knockdown did not affect viability (p>0.06 in all conditions, Student's t-test).

Figure 2-25

Figure 2-26 Tumors derived from HUWE1 knockdown cells were resistant to treatment with NVP-BEZ235 *in-vivo.* treatment with NVP-BEZ235 *in-vivo.*

HUWE1 knockdown (sh-1) or shRNA-control Kelly lines were transplanted orthotopically into renal capsules of nude mice. Daily treatment with NVP-BEZ235 (35mg/kg) or vehicle was initiated on day 14. Tumors were collected for analysis after 2 weeks of treatment. N=5 for each arm. Vehicle treated arms from both sh-control and HUWE1 knock-down lines were normalized to 100%, and NVP-BEZ treated arms were graphed as percent change compared to vehicle treated
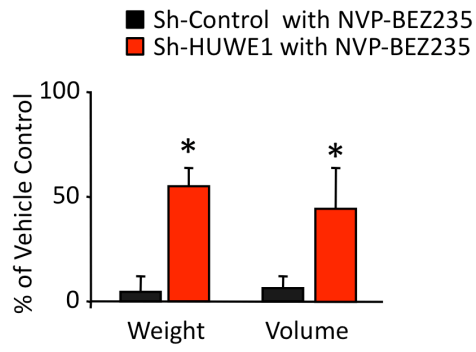
(**A**) Tumor burden (weight and volume): NVP-BEZ235 blocked shRNA-control tumors, whereas HUWE1 knockdown tumors showed significant growth despite treatment with NVP-BEZ235, (*,P< 0.003, Student's t-test, for difference).

(**B**) Representative images of whole tumors under each condition. White ovals indicate kidney in each sample. Scale bar = 5mm
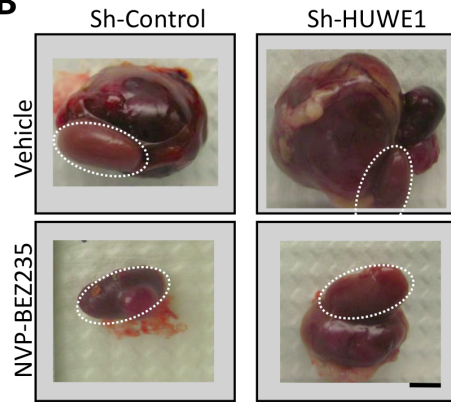
# Figure 2-26

A

Tumor burden

B

Figure 2-27 Tumor Angiogenesis and proliferation in tumors derived from HUWE1 knockdown cells conferred resistant to treatment with NVP-BEZ235.

(**A-P**) Histological analysis: CD31 (Endothelial cells). Ki67 (proliferating cells). DAPI (nuclei), and H&E. Scale bar = 50 μm

(**Q**) Quantification of data from (**C-N**). Vascular density (CD31) and proliferation (Ki67) in HUWE1 knockdown tumors were resistant to treatment with NVP-BEZ235, relative to shRNA control tumors (**P< 0.003, Student's t-test). N=3 mice in each arm. Three representative images per mouse were quantitated using ImageJ.

Figure 2-27
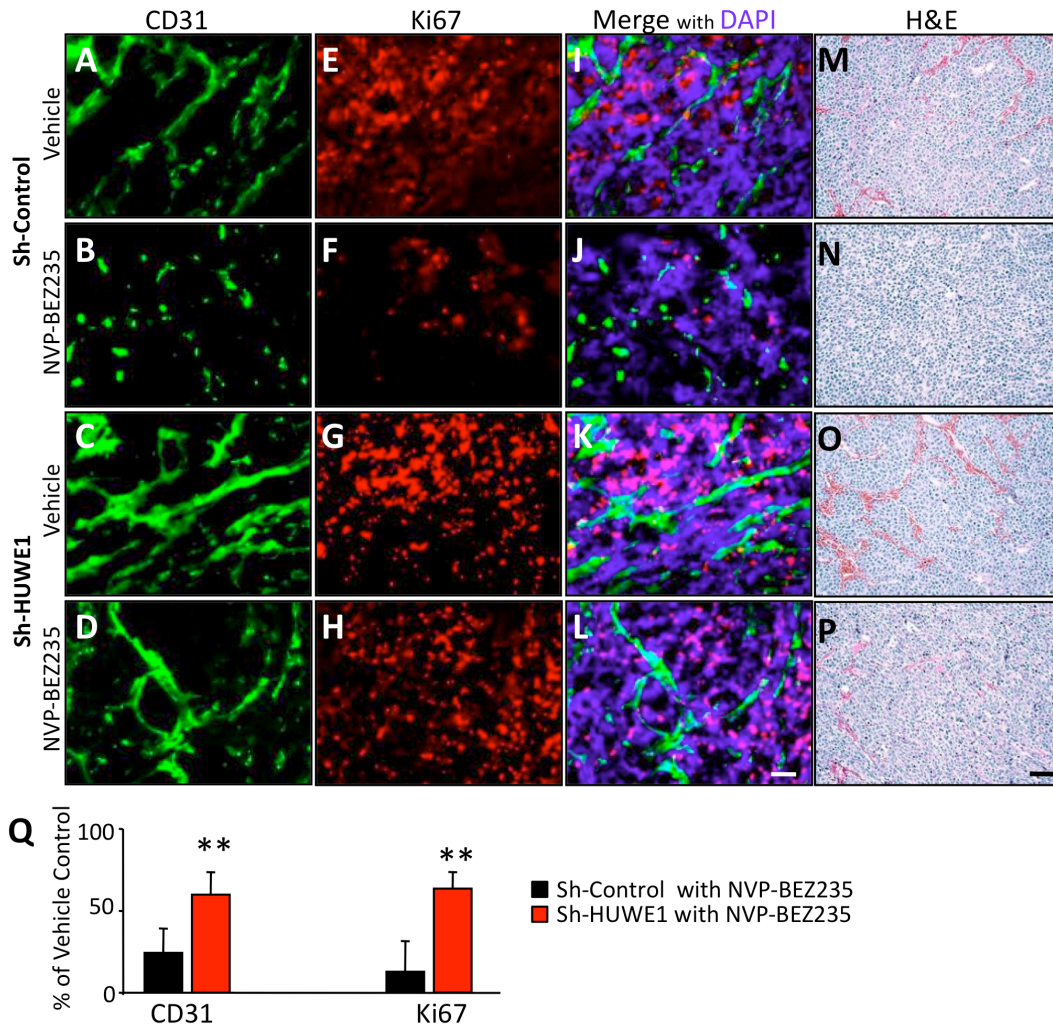
CHAPTER 3: A feed forward loop linking PI3K, microRNAs-17~92 and MYCN in neuroblastoma

Source: The following chapter contains both unpublished data, and parts of published article in Nature Medicine (PMID: 20871609)

INTRODUCTION

Neuroblastoma, a solid tumor of peripheral neural crest origin accounts for 15% of pediatric cancer deaths(*1*). Amplification of the transcription factor *MYCN* is the cardinal feature of high-risk neuroblastoma, occurs in ~25% of cases, and is associated with less than 20% survival; *MYCN*-amplification also contributes to malignancy, metastasis and resistance to conventional treatment(*1*).

Although *MYCN* activation in neuroblastoma leads to cell-cycle entry and proliferation of tumor cells (*2*); apoptosis is also driven by MYCN. Both c-myc and MYCN induce the expression of six microRNAs in the mir-17-92 cluster [miR-17, miR-18a, miR-19a, miR-19b, miR-20a, and miR-92-1 (*3*)] by binding to E-box recognition sites in the promoter of this cluster (*4, 5*). The miR-17-92 cluster is itself oncogenic, promoting cell proliferation and suppressing apoptosis (*4, 8, 9*).

Deletion of miR-17-92 in mice leads to increased level of apoptosis, small embryos and immediate postnatal death (*10*). Several pieces of evidence support a role for miRNAs as critical target genes of MYCN in neuroblastoma; First, Myc binds directly to the mir-17-92 polycistron and activates expression of miRNAs within this cluster (*6*). Second, the miR 17-92 cluster is activated in MYCN-driven neuroblastoma, with expression enriched in high-risk MYCN amplified neuroblastoma(*5*) (*4, 11*). Third, the miR-17~92 cluster can

potentially augment tumor angiogenesis by repressing apoptosis and the expression of anti-angiogenic factors (*4*).

Specific targets for individual members of miR17-92 cluster are still being determined, and to date, the functions of individual miRNAs of this cluster have not been analyzed in neuroblastoma. In this chapter, we show that MYCN protein plays an essential role in altering miRNA17~92 expression in neuroblastoma. Further, our data suggest that activation of miR-17-92 targets the lipid phosphatase *PTEN*, activates PI3K, subsequently stabilizes MYCN, and drives a feed-forward loop. A role for PTEN as a target of this cluster has also been suggested by others (*12-14*). Lastly, we show in an in-vivo efficacy study, that a novel anti-miR directed against miR-380, a candidate regulator of p53, showed activity in an orthotopic model of neuroblastoma driven by, showing the potential of anti-miR therapy for neuroblastoma treatment.

RESULTS

miR-17-92 expression correlates with MYCN level.

To examine whether levels of MYCN protein correlate with miR-17-92 expression, we tested a panel of *MYCN*-amplified and non-amplified human neuroblastoma-derived cell lines, using qRT-PCR for individual miRs (Fig. 3-1). In cells with high MYCN, the level of miR-19a was 3-5 fold higher than that observed in cells with low levels of MYCN. Similar results were observed with miR 17, 18a, 19b, 20a and 92-1 (not shown). We also used SHEP-TET21/N, a human neuroblastoma cell line in which transcription of MYCN can be toggled "off" or "on" by the addition of doxycycline (dox) to the media (Chapter 2), to verify the correlations of individual miRs with MYCN. Our data suggest that MYCN is the key regulator of miR-17~92 expression.

PI3K/mTOR inhibitor reduces mIR-19a through MYCN.

Since NVP-BEZ235 destabilizes MYCN protein in both *in vitro* and *in vivo,* we hypothesized that miR-19a may be secondarily affected by this inhibitor. As in Chapter 2 (Fig. 2-11 and 2-12), we transduced SHEP cells with retroviral vectors expressing wild-type murine MYCN *(MYCN^{WT})* or a mutationally stabilized phospho-mutant of *MYCN (MYCN^{T58A})*, resistant to NVP-BEZ235. We then analyzed the effects of NVP-BEZ235 on miR-19a by qRT-PCR. Treatment with NVP-BEZ235 significantly reduced levels of miR19a by 50% in *MYCN^{WT}* cells, with P value <0.005, as compared with 23% reduction in *MYCN^{T58A}* cells, P=0.055 (Fig. 3-2). This result suggests that MYCN protein

stability contributes to expression of miR-19a. To extend these results, we analyzed tumors from mice transgenic for TH- *MYCN* for miR-19a expression, using in-situ hybridization. NVP-BEZ235 treatment in these tumors (previously shown to suppress MYCN) led to decreased levels of miR-19a (Fig. 3-3), indicating that this PI3K/mTOR inhibitor altered miR-19a level through blockade of MYCN in-vivo.

miR-17~92 over-expression targets *PTEN*, activates PI3K, and subsequently stabilizes MYCN

Although activation of PI3K/mTOR is well characterized in neuroblastoma, the basis for this activation remains uncertain. Whereas many tumors that show activation of PI3K show either common amplification of upstream receptor tyrosine kinases, or show activating mutations in PI3K itself, neither of these mutations occurs commonly in neuroblastoma. been describe why most human *MYCN*-amplified neuroblastomas activate PI3K. Recently, PTEN has been demonstrated as a possible target of miR-19a in other cancers (*12-14*), offering a potential mechanism through which miRs could activate PI3K and further stabilize MYCN protein in neuroblastoma. To determine whether miR-17~92 overexpression could activate PI3K signaling, we therefore transduced this miR cluster into neuroblastoma cells (Fig.3-4). The results demonstrate that miR-17-92 reduced levels of PTEN, associated with activation of pAkt and increased levels of MYCN. We verified this result using additional

MYCN-amplified and non-amplified neuroblastoma cell lines, showing again, that miR-17~92 overexpression activated pAkt (Fig. 3-5). These data suggest that MYCN-induces the miR 17-92 cluster, negatively regulating PTEN, and potentially contributing both to increased levels of MYCN, and providing the PI3K-driven apoptotic blockade necessary for unregulated tumor growth and malignancy.

Knockdown of miR-19a attenuates the suppression of PTEN

Next we assessed whether knockdown of miR-19a and 19b could rescue PTEN. We therefore transfected Kelly cells with anti-sense locked nucleic acid (LNA) against miR-19a and b. Our data show that LNA-miR-19a and LNA-miR-19b effectively rescued PTEN (Fig. 3-6), suggesting that miR-19a and b are the suppressors of PTEN in neuroblastoma.

Anti-miR therapy: a proof of concept

Although microRNA antagonist deliveries in-vivo is quite challenging, the ability to administer anti-miR inhibitor therapies efficiently remains an unmet need in preclinical studies. Along with our collaborators in Goga lab at UCSF, we obtained anti-miR antagonists from Regulus Therapeutics (*15*). Together, we established an in-vivo delivery system for anti-miR therapy, using anti-miR-380 (Fig. 3-7), which rescues p53 activity in an allograft model of TH-

MYCN (*15*). The use of this allograft model allowed us to expand the number mice in the study using the same tumor with p53 wildtype status. Treatment with anti-miR-380 showed significant reduction in tumor growth as compared to control in-vivo, validating a number of in-vitro studies with this miR antagonist (Fig 3-7). Our efficacy study with anti-miR-380 provides proof of concept, allowing future use of this approach to deliver specific anti-miR therapies (including anti-miR19a) in neuroblastoma and other cancers.

DISCUSSION

In chapter 2, we demonstrated that a clinical PI3K/mTOR inhibitor can target MYCN, leading to destabilization of MYCN in both a GEM model for MYCN-driven neuroblastoma, and in primary orthotopic human neuroblastoma tumors. Although these observations suggest that PI3K contributes to MYCN stabilization in neuroblastoma tumors, common mutations for activating PI3K (such as activation of upstream RTK, activating mutations in *PI3K* or deletions in *PTEN*) are rare in neuroblastoma (*16*). Since activation of Akt is clearly correlated with low survival in this disease (*17*), these studies raise fundamental questions as to how PI3K becomes activated in neuroblastoma. Our study clarifies a role for miR-17-92 as an effector of MYCN, that activates PI3K signaling in neuroblastoma. We provide evidence for a feed-forward loop in *MYCN*-amplified neuroblastoma that induces miR17-92, which targets and suppresses PTEN, leading to activation of pAkt, and subsequent stabilization of MYCN. We verified miR-19a, a component of the miR17~92 cluster, as a key regulator of PTEN in neuroblastoma, as knockdown using LNA-anti-miR-19a led to increased levels of PTEN from this suppression.

Further, as proof of concept, we successful determine the efficacy of the newly developed anti-miR therapy in our allograft TH-*MYCN* model. In the future, we plan to use this anti-miR therapy for several MYCN-driven miR-clusters, including miR-17~92, in our GEM TH-*MYCN* and primary orthotopic

human neuroblastoma SF-NB06, to determine the in-vivo functions of these miRs in tumor progression.

MATERIALS AND METHODS

Reagents

Retroviral vectors (MSCV-PIG2 –Puro) carrying the entire miR-17-92 cluster, as well as retroviruses containing individual miRs in this cluster (from Andrei Goga). We stably transduced these constructs (and vector controls) into a panel of neuroblastoma with MYCN-amplified and non-amplified cell lines and selected with puromycin (1ug/ml).

LNA inhibitors (LNA-anti-miR19a and -19b) are commercially available (Exiqon, Denmark). LNA were transfected into cells using lipofectamine kit and protocol (Invitrogen,CA).

LNA probes for (LNA-miR19a) are commercially available. In Situ Hybridization kit was provided along with probes (Exiqon, Denmark). Western Blot: pAkt and PTEN antibodies (Cell signaling, CA), Actin (Santa Cruz,CA).

miR-17-92 Cluster Real-Time PCR Assay Kit provides probes for individual miRs in the cluster and all the materials and protocol needed to run the assay (Signosis inc, CA).

Anti-miRs: Scramble control or anti-miR (with chimeric miRNA antagonist oligomers, modified at the 2′ position of the sugar with either a fluoro or a

methoxyethyl group and a full phosphorothioate backbone) were provided by the Goga Lab-UCSF, from a collaboration with Regulus Therapeutics, San Diego.

TH-*MYCN* and Allograft mouse models

TH-*MYCN* mice with tumors were treated as described in Chapter 2. Allograft mouse model derives from the original tumor of TH-*MYCN*. Tumor pieces ($2mm^3$) from GEM TH-MYCN neuroblastoma were implanted into kidney capsule of nude mice. After 2 days, mice were treated twice weekly for 3 weeks with scramble control or anti-miR (with chimeric miRNA antagonist oligomers, modified at the 2′ position of the sugar with either a fluoro or a methoxyethyl group and a full phosphorothioate backbone, Regulus Therapeutics, San Diego). Tumors were collected at the last day of treatment, weight and volume, were recorded.

REFERENCES

1.   G. M. Brodeur, Neuroblastoma: biological insights into a clinical enigma. *Nat Rev Cancer* **3**, 203 (2003).
2.   C. Schorl, J. M. Sedivy, Loss of protooncogene c-Myc function impedes G1 phase progression both before and after the restriction point. *Mol Biol Cell* **14**, 823 (2003).
3.   V. Olive, I. Jiang, L. He, mir-17-92, a cluster of miRNAs in the midst of the cancer network. *Int J Biochem Cell Biol* **42**, 1348 (2010).
4.   M. Dews, A. Homayouni, D. Yu, D. Murphy, C. Sevignani, E. Wentzel, E. E. Furth, W. M. Lee, G. H. Enders, J. T. Mendell, A. Thomas-Tikhonenko, Augmentation of tumor angiogenesis by a Myc-activated microRNA cluster. *Nat Genet* **38**, 1060 (2006).
5.   J. H. Schulte, S. Horn, T. Otto, B. Samans, L. C. Heukamp, U. C. Eilers, M. Krause, K. Astrahantseff, L. Klein-Hitpass, R. Buettner, A. Schramm, H. Christiansen, M. Eilers, A. Eggert, B. Berwanger, MYCN regulates oncogenic MicroRNAs in neuroblastoma. *Int J Cancer* **122**, 699 (2008).
6.   J. T. Mendell, miRiad roles for the miR-17-92 cluster in development and disease. *Cell* **133**, 217 (2008).
7.   G. Stefani, F. J. Slack, Small non-coding RNAs in animal development. *Nat Rev Mol Cell Biol* **9**, 219 (2008).
8.   L. He, J. M. Thomson, M. T. Hemann, E. Hernando-Monge, D. Mu, S. Goodson, S. Powers, C. Cordon-Cardo, S. W. Lowe, G. J. Hannon, S. M. Hammond, A microRNA polycistron as a potential human oncogene. *Nature* **435**, 828 (2005).
9.   K. A. O'Donnell, E. A. Wentzel, K. I. Zeller, C. V. Dang, J. T. Mendell, c-Myc-regulated microRNAs modulate E2F1 expression. *Nature* **435**, 839 (2005).
10.   A. Ventura, A. G. Young, M. M. Winslow, L. Lintault, A. Meissner, S. J. Erkeland, J. Newman, R. T. Bronson, D. Crowley, J. R. Stone, R. Jaenisch, P. A. Sharp, T. Jacks, Targeted deletion reveals essential and overlapping functions of the miR-17 through 92 family of miRNA clusters. *Cell* **132**, 875 (2008).
11.   Y. Chen, R. L. Stallings, Differential patterns of microRNA expression in neuroblastoma are correlated with prognosis, differentiation, and apoptosis. *Cancer Res* **67**, 976 (2007).
12.   B. P. Lewis, I. H. Shih, M. W. Jones-Rhoades, D. P. Bartel, C. B. Burge, Prediction of mammalian microRNA targets. *Cell* **115**, 787 (2003).
13.   S. Takakura, N. Mitsutake, M. Nakashima, H. Namba, V. A. Saenko, T. I. Rogounovitch, Y. Nakazawa, T. Hayashi, A. Ohtsuru, S. Yamashita, Oncogenic role of miR-17-92 cluster in anaplastic thyroid cancer cells. *Cancer Sci* **99**, 1147 (2008).
14.   V. Olive, M. J. Bennett, J. C. Walker, C. Ma, I. Jiang, C. Cordon-Cardo, Q. J. Li, S. W. Lowe, G. J. Hannon, L. He, miR-19 is a key oncogenic component of mir-17-92. *Genes Dev* **23**, 2839 (2009).

15. A. Swarbrick, S. L. Woods, A. Shaw, A. Balakrishnan, Y. Phua, A. Nguyen, Y. Chanthery, L. Lim, L. J. Ashton, R. L. Judson, N. Huskey, R. Blelloch, M. Haber, M. D. Norris, P. Lengyel, C. S. Hackett, T. Preiss, A. Chetcuti, C. S. Sullivan, E. G. Marcusson, W. Weiss, N. L'Etoile, A. Goga, miR-380-5p represses p53 to control cellular survival and is associated with poor outcome in MYCN-amplified neuroblastoma. *Nat Med* **16**, 1134).

16. W. C. Gustafson, W. A. Weiss, Myc proteins as therapeutic targets. *Oncogene* **29**, 1249).

17. D. Opel, C. Poremba, T. Simon, K. M. Debatin, S. Fulda, Activation of Akt predicts poor outcome in neuroblastoma. *Cancer Res* **67**, 735 (2007).

18. A. Swarbrick, S. L. Woods, A. Shaw, A. Balakrishnan, Y. Phua, A. Nguyen, Y. Chanthery, L. Lim, L. J. Ashton, R. L. Judson, N. Huskey, R. Blelloch, M. Haber, M. D. Norris, P. Lengyel, C. S. Hackett, T. Preiss, A. Chetcuti, C. S. Sullivan, E. G. Marcusson, W. Weiss, N. L'Etoile, A. Goga, miR-380-5p represses p53 to control cellular survival and is associated with poor outcome in MYCN-amplified neuroblastoma. *Nat Med* **16**, 1134 (2010).

19. S. Fulda, W. Lutz, M. Schwab, K. M. Debatin, MycN sensitizes neuroblastoma cells for drug-induced apoptosis. *Oncogene* **18**, 1479 (1999).

FIGURE LEGENDS:

Figure 3-1. MYCN protein activates miRs in the miR-17-92 cluster

Real time-PCR analysis measuring levels of miR-19a.

In MYCN-driven SHET-TET21/N "on" and Kelly, miR19a level is 3 to 5 fold higher than in low MYCN SHEP, SKNSH, and SHEP-TET21/N "off". Similar results were obtained for other members of the cluster: miR-17, miR-18a, miR-19b, miR-20a, and miR-92-1 (not shown).
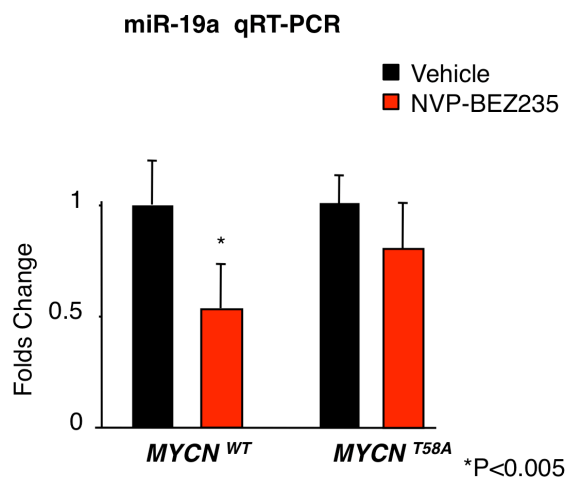
Figure 3-1

miR-19a qRT-PCR

■ Low MYCN
■ High MYCN

*P<0.005
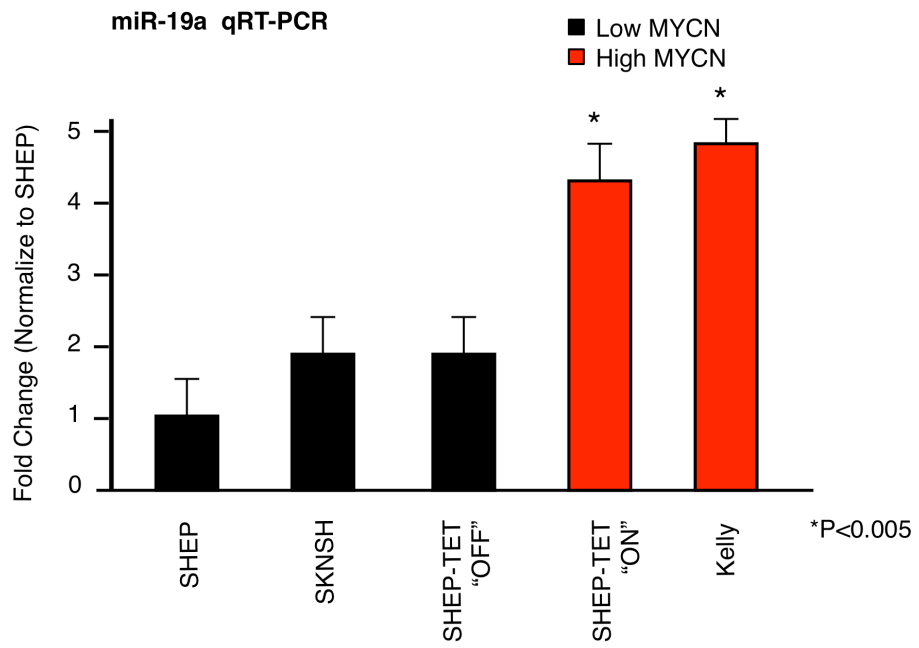
Figure 3-2. A dual PI3K/mTOR inhibitor reduces miR19a through suppression of MYCN.

SHEP cells transduced with pLenti6.3 *MYCN^{WT}* or *MYCN^{T58A}* constructs as described in Chapter 2. *MYCN^{WT} and MYCN^{T58A}* cells were treated with vehicle or NVP-BEZ235 for 48h.

Real time-PCR analysis (mIR19a): NVP-BEZ235 treatment led to decreased levels of miR-19a in *MYCN^{WT}* and was blunted in the *MYCN^{T58A}*

Figure 3-2

miR-19a qRT-PCR

■ Vehicle
■ NVP-BEZ235

*P<0.005

Figure 3-3. NVP-BEZ235 treatment in-vivo decreases levels of miR-19a.

Tumors from mice transgenic for TH-*MYCN* were treated with NVP-BEZ235 (35mg/kg) or PEG-300 vehicle once daily by oral gavage, and mice were sacrificed at 14d of treatment.

(**A**) In-situ hybridization: Tumor were perfusion fixed, and analyzed by using a locked nucleic acid (LNA) DIG-tagged probe for anti-sense to mir-19a, detected by anti-DIG-Cy3.
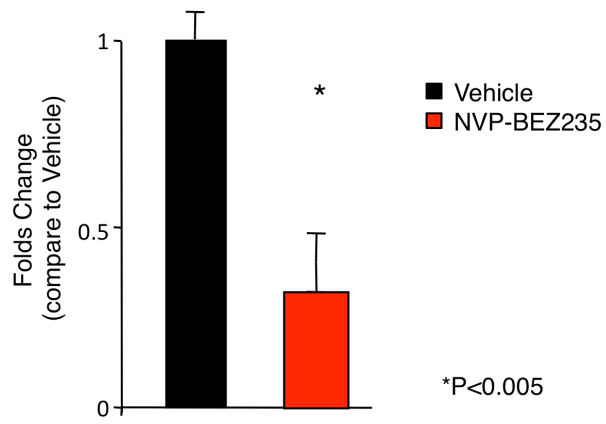
(**B**) Quantitations of (**A**) Three representative images per mouse were quantitated using imageJ.

Figure 3-3

A

Vehicle   NVP-BEZ235

miR-19a/ Anti-DIG-Cy3 & DAPI

B

*P<0.005
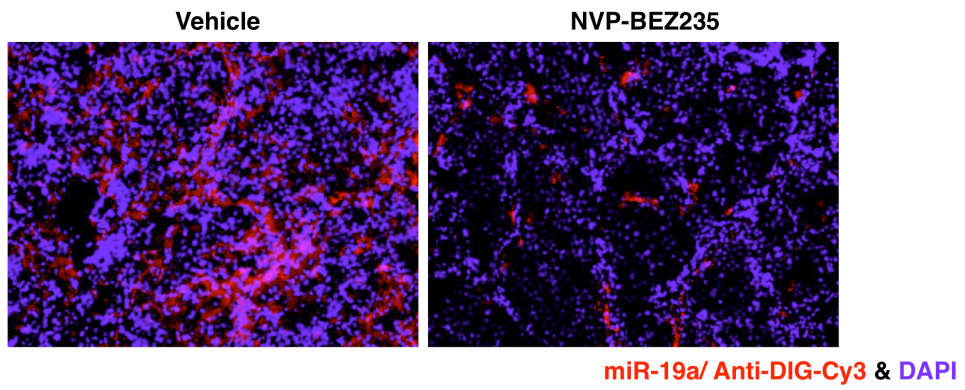
Figure 3-4. mIR-17~92 cluster targets PTEN, allows activation of pAkt, and stabilizes MYCN in neuroblastoma cells.

Kelly cells were stably transduced with MSCV empty vector control or miR-17-92 cluster, and selected using puromycin.

Western Blot: Immunoblot demonstrating that forced expression of the miR-17-92 cluster in Kelly cells led to decreased levels of PTEN, associated with activation of pAkt, and stabilization of MYCN.
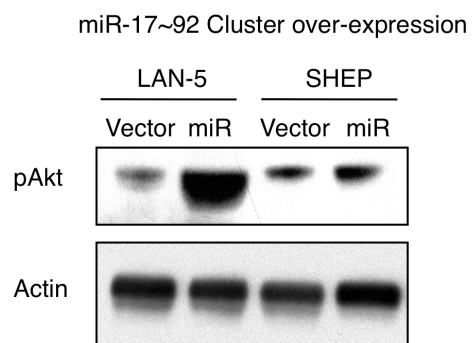
Figure 3-4
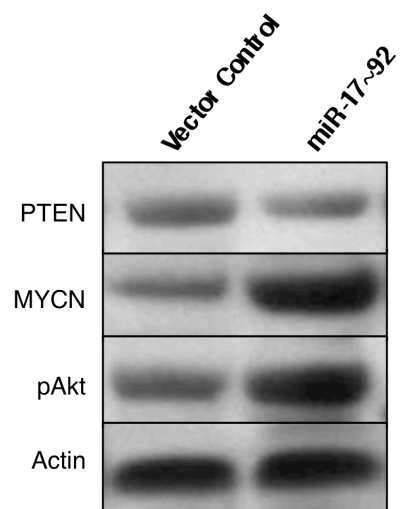
Figure 3-5. Over-expression of miR-17~92 cluster elevates pAkt in both MYCN-amplified and non-amplified neuroblastoma cells.

LAN-5 (MYCN-amplified) and SHEP (non-amplified) were stably transduced with MSCV empty vector control or miR-17-92 cluster, and selected using puromycin.

Western Blot: Over-expression of miR cluster induces pAkt in both cell lines. However, the level of pAkt induction is higher in LAN5 than in SHEP cells.
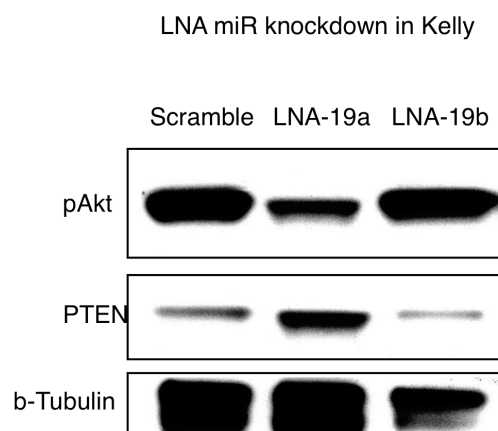
Figure 3-5

Figure 3-6. miR-19a knockdown restores PTEN expression

Kelly cells were transfected with either locked nucleic acid (LNA) probe anti-sense to mir-19a or scramble control.

Western Blot: LNA-miR-19a is more effective than LNA-miR-19b in restoring PTEN-function, leading to reduction of pAkt.

Figure 3-6

LNA miR knockdown in Kelly

Scramble   LNA-19a   LNA-19b

pAkt

PTEN

b-Tubulin

Figure 3-7. The efficacy of anti-miR in vivo therapy in neuroblastoma: a proof of concept

Tumor pieces ($2mm^3$) from TH-MYCN were transplanted into renal capsule of nude mice to generate an allograft model of neuroblastoma. Two days after the initial transplants, mice where treated with miR-380 antagonist or scramble control for 21d. Tumors were then extracted from the mice.

(A) Representative images of the whole tumors from miR-380 antagonist or control. Scale bars-1 cm.

(B) Tumor mass (g): miR-380 antagonist inhibits tumor growth (n=5 mice per group, *$P < 0.01$, student's t-test). Weight of the kidney represents as dashed red line.

Figure 3-7

A

Control

Anti-miR-380

B
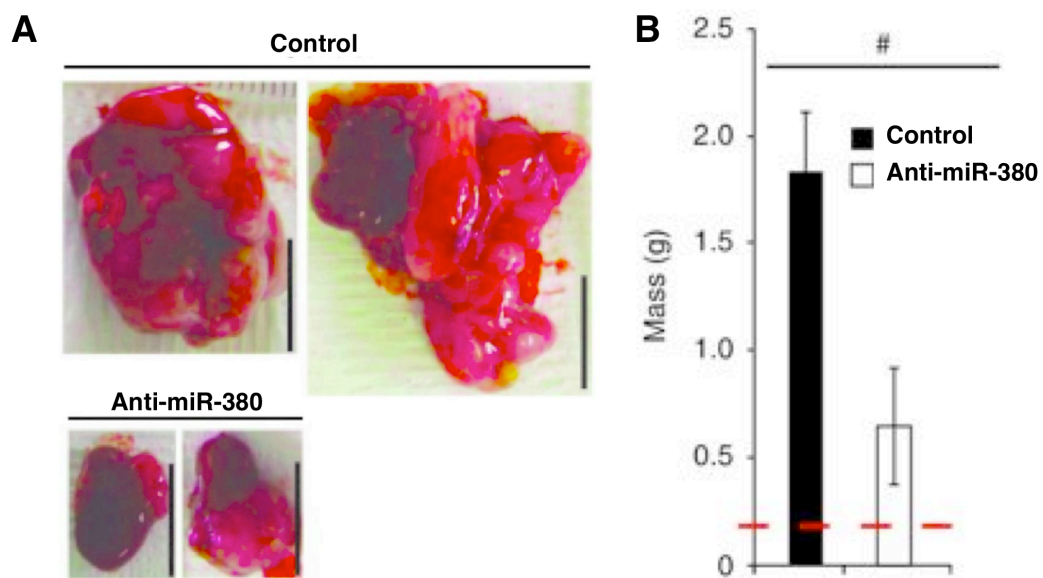
CHAPTER 4: CONCLUSION

MYCN protein plays an essential role in neuroblastoma malignancy, and usually associates with poor outcomes. MYCN also represents an attractive therapeutic target because of its function in the tumor-microenvironment and the post-transcriptional regulations of signal transduction. Our findings provide evidence that MYCN protein is stabilized through PI3K/mTOR signaling pathway. Clinical inhibitor NVP-BEZ235 blocks both neuroblastoma tumor cells and endothelial cells in the tumor-vascular microenvironment by affecting MYCN stability. Further, in this work, we determine MYCN as a biomarker for the efficacy of PI3K/mTOR inhibitor; targeting MYCN improves survival in TH-MYCN and orthotopic human primary MYCN-amplified models, reducing tumor burdens in both models. Using multiple approaches (PI3K-resistant alleles $MYCN^{T58A}$, shRNA against $MYCN$, a doxycycline-repressible allele of MYCN, and shRNA against the ubiquitin ligase) we have further established that the action of NVP-BEZ235 on tumor cells leads to decreased level of VEGF mRNA, and decreased density of endothelial cells through this paracrine signaling mechanism.

These initial findings clarify the role for PI3K/mTOR on stabilization of MYCN protein. However, it remains an important question how most $MYCN$-amplified neuroblastomas activate PI3K signaling in the first place. Our study provides several important answers, describing the role for miR-17-92, a microRNA cluster induced by MYCN, as a post-transcriptional activator of PI3K signaling

in neuroblastoma. Our data suggest that miR-19a targets *PTEN*, activating PI3K, stabilizing MYCN, and driving a feed-forward loop. We then use LNA-anti-miR-19a and 19b approaches in cell lines to rescue *PTEN* and antagonize the functions of these miRs. In addition, for the first time, we successfully evaluate the efficacy of the new anti-miR therapy, using the orthotopic allograft model of TH-*MYCN*, showing reduction of tumor burdens in-vivo.

In the future, we anticipate the use of anti-miR-19a therapy, along with other specific anti-miRs against the members of miR-17~92, in MYCN-driven tumors. GEM mouse model TH-*MYCN (spontaneous tumors)*, and orthotopic model of human primary *MYCN*-amplified SFNB-06 neuroblastoma will be used to evaluate the preclinical efficacy of this therapy, by determining the pathohistological changes, overall survival and tumor progression. It is one of our interests to also combine anti-miRs with PI3K/mTOR inhibitors to determine whether the combinations would provide synergistic responses in tumors. Altogether, it is our ultimate goal to use the anti-miR therapy, along with the GEM, allograft model of *TH-MYCN* and orthotopic models of human primary neuroblastoma, as the foundation to identify new targets and new therapies for neuroblastoma and other MYCN-driven cancers.
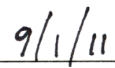
Library Release

Publishing Agreement

It is the policy of the University to encourage the distribution of all theses, dissertations, and manuscripts. Copies of all UCSF theses, dissertations, and manuscripts will be routed to the library via the Graduate Division. The library will make all theses, dissertations, and manuscripts accessible to the public and will preserve these to the best of their abilities, in perpetuity.

Please sign the following statement:

I hereby grant permission to the Graduate Division of the University of California, San Francisco to release copies of my thesis, dissertation, or manuscript to the Campus Library to provide access and preservation, in whole or in part, in perpetuity.

_____   _____
Author Signature   9/1/11
                                                                          Date